
Supporting Information

Improved affinity: A customized fluorescent probe for the rapid detection of butyrylcholinesterase

Wei Wang ^{1,2}, Xiao-Fei Chen ^{1,2}, Yi Zhang ³, Yang Ran ^{1,2}, Long Jin ^{1,2}, Shuai Li ^{4,*} and Bai-Ou Guan ^{1,2,*}

¹ Guangdong Provincial Key Laboratory of Optical Fiber Sensing and Communication, Institute of Photonics Technology, Jinan University, Guangzhou 510632, China;

² College of Physics & Optoelectronic Engineering, Jinan University, Guangzhou 510632, China.

³ College of Life Science and Technology, Jinan University, Guangzhou 510632, China;

⁴ Special Needs Medical Center, The Eighth Affiliated Hospital of Sun Yat-sen University, Shenzhen 518033, China;

* Correspondence: tguanbo@jnu.edu.cn (B.-O. G.), Tel.: +86-20-37337012; lish398@mail.sysu.edu.cn (S. L.)

Contents

1. Experimental details.....	2
2. Figures S1–S9.....	3
3. Table S1	8
4. Synthesis details and characterizations.....	9
5. NMR Spectra	14
6. Reference.....	32

1. Experimental details

1.1 Materials and instruments

Cyclopropylcarbonyl chloride was purchased from Yien Chemical Co., Ltd. (Shanghai, China); malononitrile and anhydrous sodium sulfate were obtained from Macklin Biochemical Co., Ltd.; hydrochloric acid, ether, dichloromethane, ethyl acetate, toluene, ethanol, and acetonitrile were sourced from Guangte Reagent Technology Co., Ltd. (Guangzhou, China); butyrylcholinesterase (10 U/mg) was purchased from Sigma-Aldrich (St. Louis, MO, USA)—50 $\mu\text{g/mL}$ corresponds to 0.5 U/mL; acetylcholinesterase and carboxylesterase were purchased from Shanghai Yuanye Biotechnology. 3-Chloro-4-hydroxybenzaldehyde and 2,3,3-trimethyl-4,5-benzindole were purchased from Shanghai Bide Pharmaceutical Technology Co., Ltd. (Shanghai, China); tetrahydrofuran, sodium hydride, triethylamine, iodomethane, sodium tert-butoxide, 1,4-butanedisulfone, and iodoethane were sourced from Shanghai San Chemical Co., Ltd. (Shanghai, China). 2-Methylquinoline-2'-hydroxyphenylketone and dimethylamine were purchased from Shanghai Mayer Chemical Co., Ltd. (Shanghai, China). All solvents and reagents were commercially available and did not require further purification.

Absorption spectra were recorded using a UV-visible spectrophotometer (Techcomp, UV2310). Fluorescence measurements were conducted on a spectrophotometer (Ocean Insight, QE Pro-Raman) using a 1×10 mm quartz cell with a 5 nm slit width, excited by a xenon lamp source (Zolix, Gloria-X150A). Cell images were captured using a laser confocal microscope (Leica, SP8). Cell viability was assessed with an ELISA reader (TECAN, Spark 10M). ^1H and ^{13}C nuclear magnetic resonance spectra in CDCl_3 (with TMS as the internal standard) or $\text{DMSO-}d_6$ were recorded on a Bruker 600 MHz spectrometer. Mass spectrometry was performed using a high-resolution mass spectrometer (SCHEX, AB SCIEX 500R).

1.2 Calculation of detection limit

Based on the linear relationship between fluorescence intensity and BChE concentration in Figure 5B, the limit of detection was calculated by the following formula: detection limit = $3\sigma/k$. σ is the standard deviation of the blank measurement and k is the slope of the fluorescence intensity versus different BChE concentrations.

1.3 Calculation of fluorescence quantum yield (Φ)

Rhodamine B was used as the reference standard (Φ_{stand} is 0.97 in ethanol) in measuring the fluorescence quantum yield. The absorption and fluorescence spectra of the product **FL** resulting from the hydrolysis of **P5** by BChE were measured in methanol in the 1 cm quartz cuvette. The sample's quantum yield was calculated using the following formula:

$$\Phi_{\text{samp}} = \Phi_{\text{stand}} \times \left(\frac{n_{\text{samp}}}{n_{\text{stand}}}\right)^2 \times \left(\frac{A_{\text{stand}}}{A_{\text{samp}}}\right) \times \left(\frac{F_{\text{samp}}}{F_{\text{stand}}}\right)$$

where F represents the integrated fluorescence spectra after correction; A represents the optical density; n represents the solvent refractive index [1]. The spectral data related to the calculation of quantum yield are shown in Figure S2. Rhodamine B: $\Phi_{\text{stand}} = 0.97$, $n_{\text{stand}} = 1.3626$, $A_{\text{stand}} = 0.1011$, $F_{\text{stand}} = 665.25$. Probe **P5**: $n_{\text{samp}} = 1.3359$, $A_{\text{samp}} = 0.1004$, $F_{\text{samp}} = 2.35$. Probe **P5** with BChE: $n_{\text{samp}} = 1.3356$, $A_{\text{samp}} = 0.289$, $F_{\text{samp}} = 71.82$.

1.4 Enzyme activity inhibition experiment

The inhibitory effect of Tacrine on the enzyme activity was determined by the following procedures: Incubate different concentrations of Tacrine (0, 10, 20, 30, 40, 50, 60, 70, 80, 90, 100, 150, 200 nM) with 50 $\mu\text{g/mL}$ BChE in 2 mL PBS buffer for 30 minutes, then incubate with **P5** (5 μM) for 10 minutes before measuring the fluorescence spectra of the solution. Calculate the percentage inhibition in the presence of different concentrations of Tacrine using the following formula:

$$\text{Inhibition efficiency (\%)} = \left(\frac{F_0 - F_1}{F_0} \right) \times 100\%$$

F_0 and F_1 represent the fluorescence intensity of the solution without Tacrine and with Tacrine, respectively [2].

2. Figures S1–S9

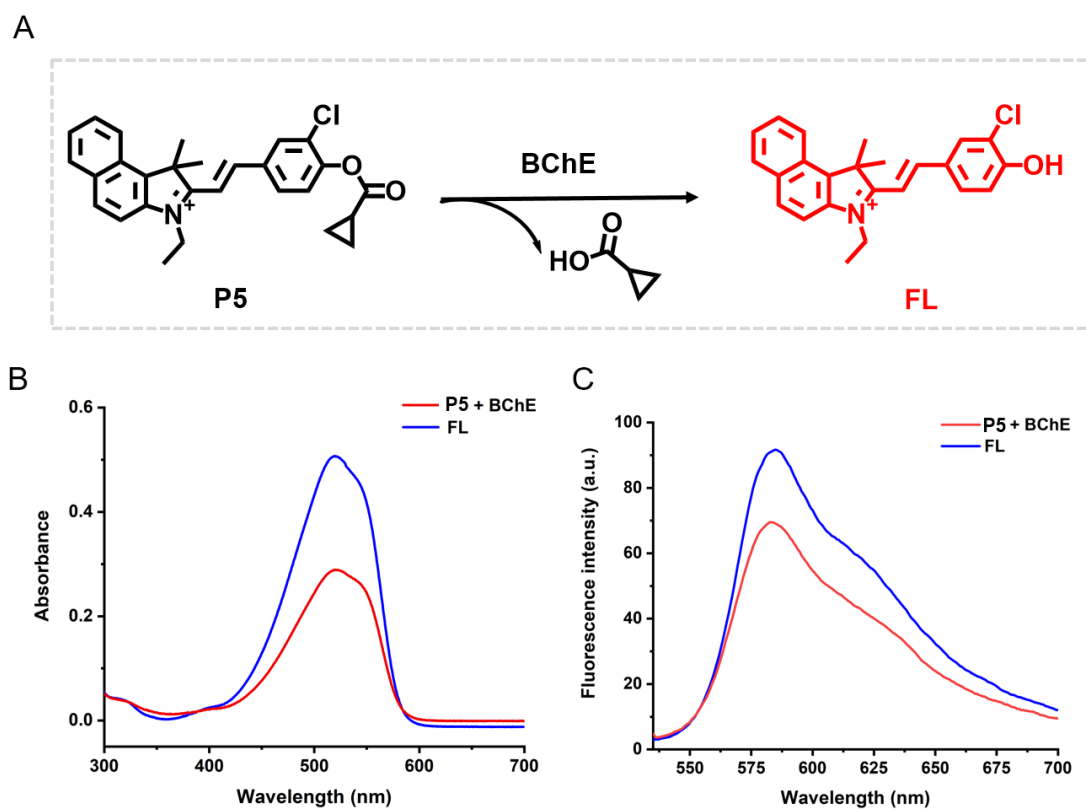


Figure S1. (A) The chemical structural changes of probe **P5** before and after response with BChE. Following the incubation of probe **P5** (5 μM) with BChE (50 $\mu\text{g}/\text{mL}$) reaction at 37 $^{\circ}\text{C}$ in 0.1 M PBS buffer (pH = 7.4) for 10 minutes, absorption spectra (B) and fluorescence spectra (C) of the reaction mixture (red line) were compared with the fluorophore **FL** (blue line). $\lambda_{\text{ex}} = 520 \text{ nm}$.

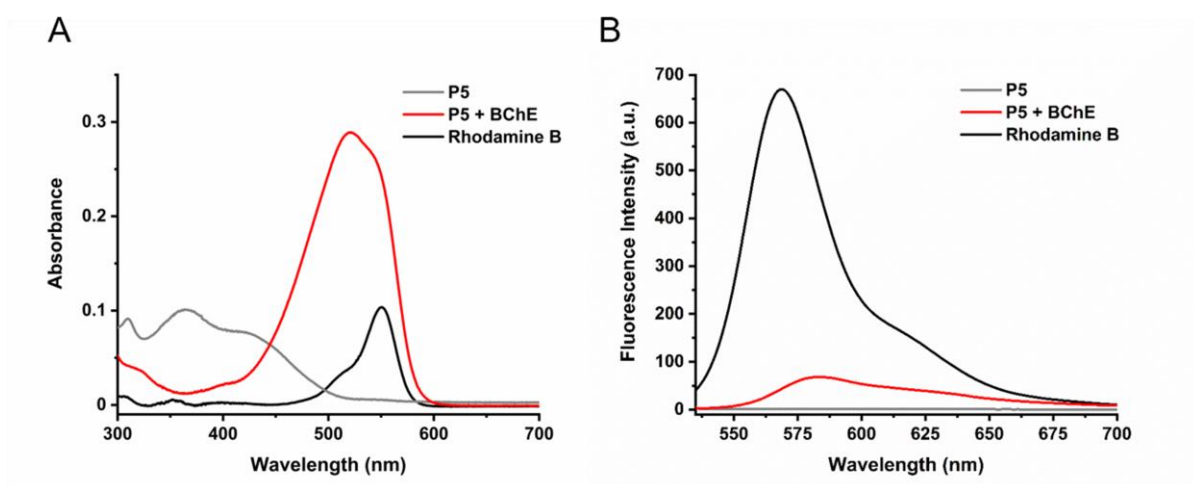


Figure S2. Absorption spectra (A) and fluorescence spectra (B) of only probe **P5** (gray line; 5 μ M), probe **P5** (5 μ M) after reacting with 50 μ g/mL BChE (red line), and Rhodamine B (black line; 5 μ M).

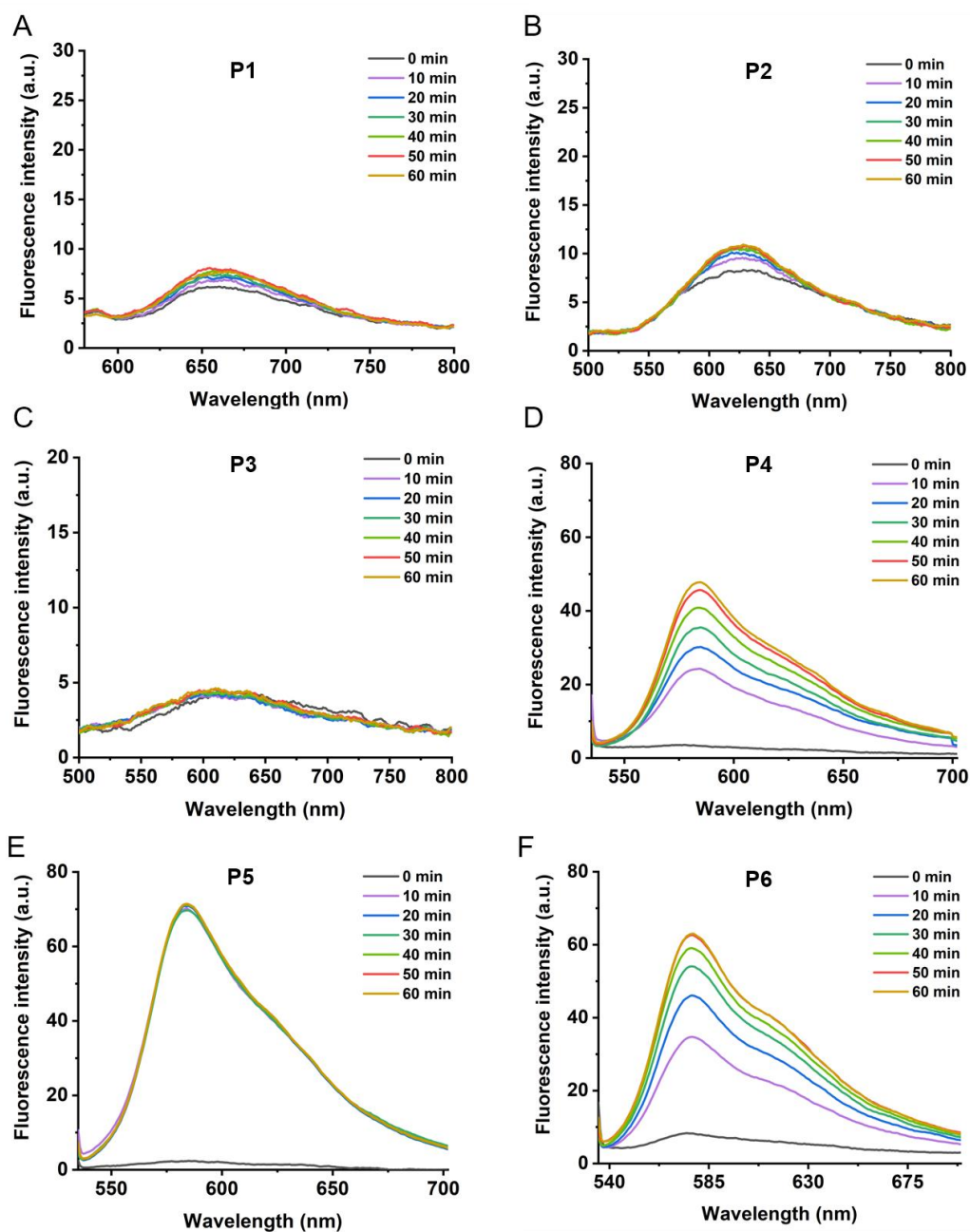


Figure S3. Fluorescence response of probes **P1**–**P6** (5 μ M) and BChE (50 μ g/mL) within 60 minutes in 0.1 M PBS buffer (pH = 7.4) at 37 $^{\circ}$ C. (A) Probe **P1**, (B) Probe **P2**, (C) Probe **P3**, (D) Probe **P4**, (E) Probe **P5**, (F) Probe **P6**.

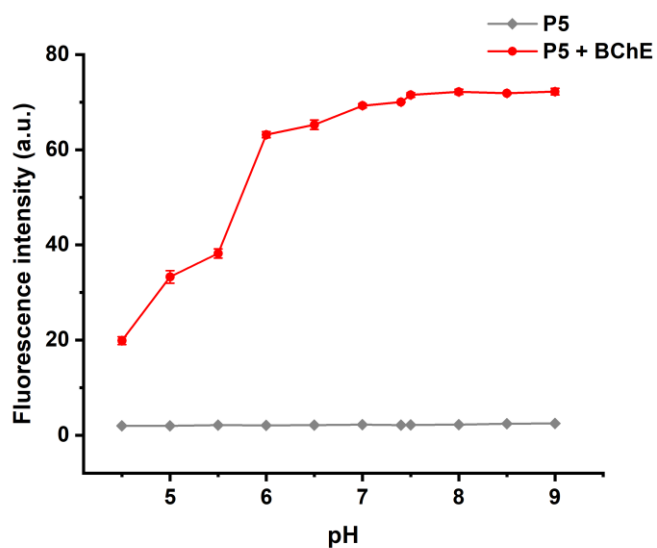


Figure S4. Fluorescence intensity at 584 nm of the reaction between probe **P5** (5 μM) and BChE (50 $\mu\text{g}/\text{mL}$) in 0.1 M PBS buffer at pH 4.5–9, before and after a 10-minute incubation at 37 $^{\circ}\text{C}$. $\lambda_{\text{ex}} = 520 \text{ nm}$.

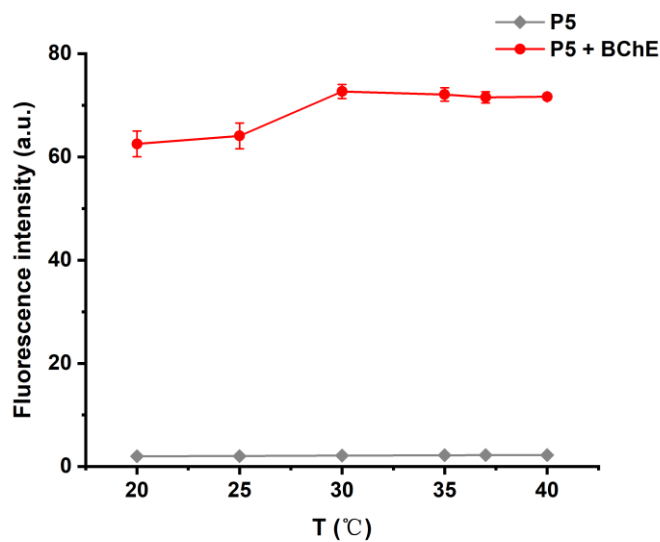


Figure S5. Fluorescence intensity at 584 nm of the reaction between probe **P5** (5 μM) and BChE (50 $\mu\text{g}/\text{mL}$) in 0.1 M PBS buffer at pH 7.4, before and after a 10-minute incubation at temperatures of 20–40 $^{\circ}\text{C}$. $\lambda_{\text{ex}} = 520 \text{ nm}$.

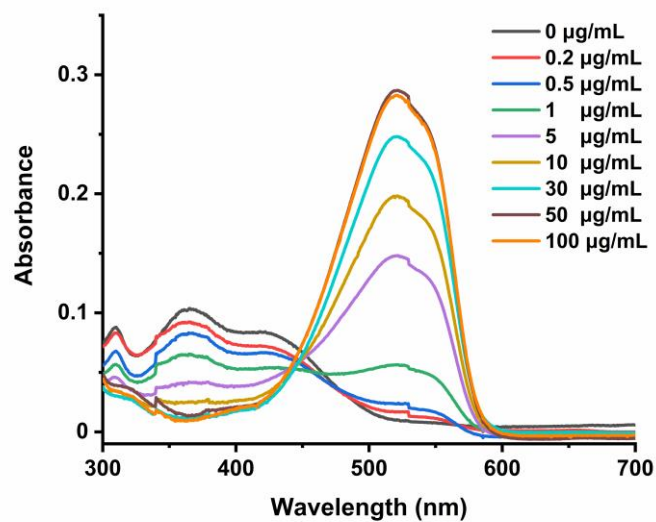


Figure S6. Absorption spectra of probe **P5** (5 μM) with BChE (0–100 μg/mL) after 10 minutes of reaction in 0.1 M PBS (pH 7.4) at 37 °C.

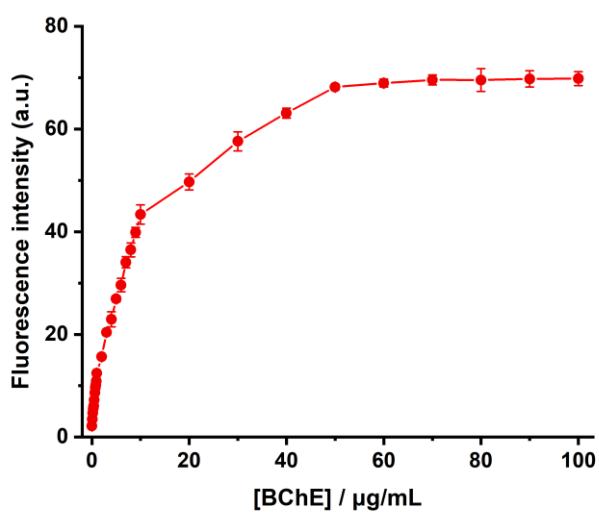


Figure S7. Fluorescence intensity curve at 584 nm of the reaction between probe **P5** (5 μM) and BChE (0–100 μg/mL) after the 10-minute reaction in 0.1 M PBS buffer (pH 7.4) at 37 °C.

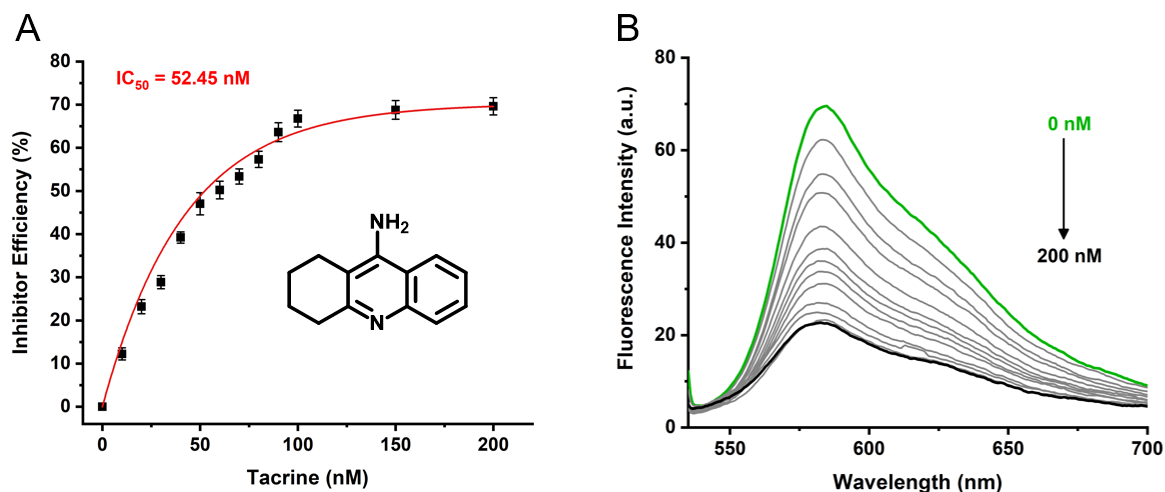


Figure S8. (A) Inhibition efficiency curve of Tacrine towards BChE, with an IC_{50} value of 52.45 nM. (B) Fluorescence spectra of probe **P5** incubated with BChE (50 $\mu\text{g}/\text{mL}$) pre-treated with different concentrations of Tacrine (0–200 nM) at 37 $^{\circ}\text{C}$ in 0.1 M PBS buffer (pH = 7.4) for 10 minutes.

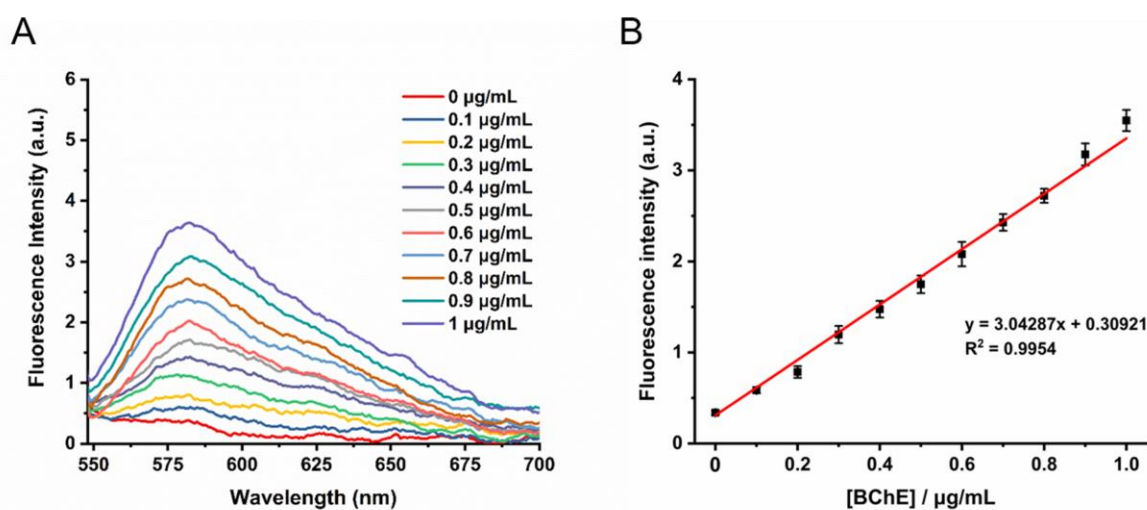


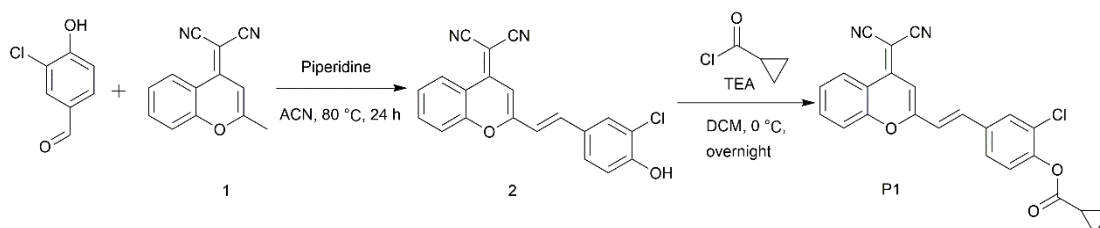
Figure S9. (A) Fluorescence spectra of probe **P5** (1 μM) with BChE (0–1 $\mu\text{g}/\text{mL}$) after 10 minutes of reaction in 0.1 M PBS (pH 7.4) at 37 $^{\circ}\text{C}$. (B) The fitted curve of the fluorescence intensity of probe **P5** (1 μM) at 584 nm with BChE concentrations ranging from 0 to 1 $\mu\text{g}/\text{mL}$.

3. Table S1

Table S1. Reported fluorescence probes for BChE.

Probe	Reaction time	Detection limit	$\lambda_{ex}/\lambda_{em}$ (nm)	Application	Reference
Probe 1	30 min	/	355 / 525	/	[3]
BChE-FP	30 min	/	455 / 515	Cell	[4]
BChE-NIRFP	24 min	/	665 / 750	Cell, zebrafish, AD model mice	[5]
DCPDA	30 min	0.06 U/L	340 / 460	/	[6]
CyCICP	About 35 min	3.75 U/L	670 / 708	Cell	[2]
BChE-NBD	5 min	29 ng/mL	580 / 628	Cell, zebrafish, mice	[7]
Probe P1	90 min	0.075 μ g/mL	480 / 528	Cell, mice	[8]
P2	About 80 min	1.08 μ g/mL	600 / 690	Cell, AD model mice	[9]
W1	40 min	0.077 μ g/mL	416 / 446	Cell	[10]
TB-BChE	About 15 min	39.24 ng/mL	575 / 626	Cell, mice	[11]
Chy-1	5 min	0.12 ng/mL	670 / 715	Cell, AD model mice	[12]
Re-BChE	20 min	19.9 μ g/m	405 / 600	/	[13]
IND-BChE	9 min	0.63 mU/mL	400 / 505	/	[14]
P5	5 min	16.7 ng/mL	520 / 584	AD model cell	This work

4. Synthesis details and characterizations

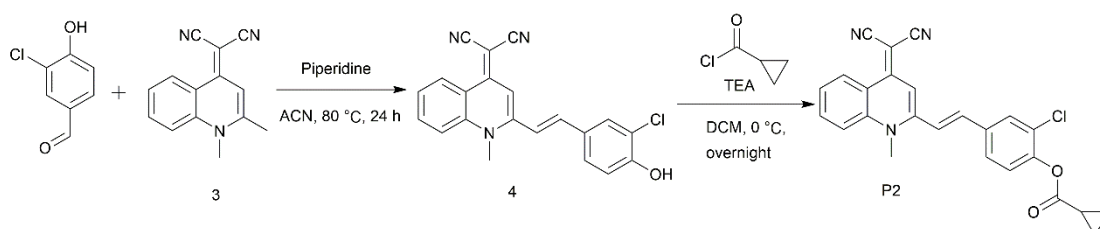


Scheme S1: Synthetic route for probe P1.

Compound 1 was synthesized according to the methods described in the literature [15].

Compound 2: Compound 1 (624 mg, 3 mmol) and 3-chloro-4-hydroxybenzaldehyde (312 mg, 2 mmol) were dissolved in acetonitrile (10 mL) and 0.5 mL of piperidine was added. The reaction mixture was heated to 80°C under argon protection and stirred for 24 hours. After the reaction was complete, the solvent was removed under vacuum and the residue was diluted with water and extracted with ethyl acetate (3 × 10 mL). The organic layer was dried over anhydrous sodium sulfate. The solution was concentrated under reduced pressure and purified by silica gel column chromatography (DCM:MeOH = 100:1) to yield a yellow solid (compound 2) of 452 mg (yield: 65%). ¹H NMR (600 MHz, DMSO-*d*₆) δ 10.93 (s, 1H), 8.73 (d, *J* = 8.3 Hz, 1H), 7.93 (t, *J* = 7.8 Hz, 1H), 7.87 (s, 1H), 7.77 (d, *J* = 8.4 Hz, 1H), 7.67 (d, *J* = 16.0 Hz, 1H), 7.62 (t, *J* = 7.8 Hz, 1H), 7.56 (d, *J* = 8.5 Hz, 1H), 7.39 (d, *J* = 16.0 Hz, 1H), 7.04 (d, *J* = 8.4 Hz, 1H), 6.98 (s, 1H). ¹³C NMR (151 MHz, DMSO-*d*₆) δ 158.89, 155.67, 153.39, 152.48, 138.09, 135.87, 129.97, 129.39, 127.88, 126.61, 125.11, 121.14, 119.47, 118.03, 117.58, 117.42, 116.40, 106.72, 60.16. HRMS (ESI): *m/z* calculated for C₂₀H₁₂ClN₂O₂⁺: 347.0587 [*M*+H]⁺, found: 347.0582.

Compound P1: Compound 2 (123 mg, 0.5 mmol) was dissolved in dry dichloromethane (10 mL). Under ice bath conditions, 0.8 mL of triethylamine was added followed by the slow addition of cyclopropylcarbonyl chloride (0.45 mL, 5 mmol). After stirring the mixture at 0 °C for 2 hours, it was allowed to react overnight at room temperature. Upon completion of the reaction, the solvent was removed under vacuum, and the residue was dissolved in ethyl acetate (15 mL). The solution was washed three times with brine, and the organic layer was dried over anhydrous sodium sulfate. The mixture was concentrated under reduced pressure and purified by silica gel column chromatography (DCM:MeOH = 100:1) to yield a pale yellow solid (compound P1) of 185 mg (yield: 89%). ¹H NMR (600 MHz, DMSO-*d*₆) δ 8.74 (d, *J* = 8.4 Hz, 1H), 8.05 (s, 1H), 7.95 (t, *J* = 7.8 Hz, 1H), 7.81–7.72 (m, 3H), 7.64 (d, *J* = 8.3 Hz, 1H), 7.63–7.59 (d, 1H), 7.43 (d, *J* = 8.4 Hz, 1H), 7.05 (s, 1H), 1.99 (m, 1H), 1.16–1.11 (m, 2H), 1.11–1.07 (m, 2H). ¹³C NMR (151 MHz, DMSO-*d*₆) δ 172.33, 157.97, 153.40, 152.45, 147.90, 136.41, 136.08, 135.08, 129.44, 128.73, 127.27, 126.76, 125.34, 125.16, 121.83, 119.52, 117.55, 116.15, 107.88, 61.47, 12.89, 9.79. HRMS (ESI): *m/z* calculated for C₂₄H₁₅ClN₂O₃⁺: 415.0849 [*M*+H]⁺, found: 415.0848.

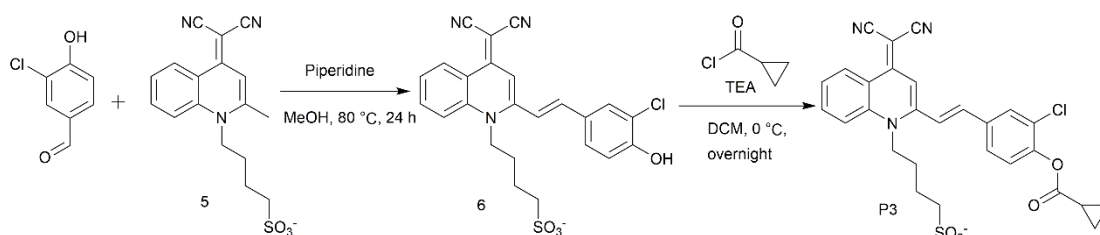


Scheme S2: Synthetic route for probe P2.

Compound 3 was synthesized according to the methods described in the literature [16,17].

Compound 4: Compound 3 (624 mg, 3 mmol) and 3-chloro-4-hydroxybenzaldehyde (312 mg, 2 mmol) were dissolved in acetonitrile (10 mL) with the addition of 0.5 mL of piperidine. Under argon protection, the reaction mixture was heated to 80 °C and stirred for 24 hours. Upon completion of the reaction, the solvent was removed under vacuum and the residue was diluted with water and extracted with ethyl acetate (3 × 10 mL). The organic layer was dried over anhydrous sodium sulfate. The solution was concentrated under reduced pressure and purified by silica gel column chromatography (DCM:MeOH = 100:1) to obtain a yellow solid (compound 4) of 452 mg (yield: 65%). ¹H NMR (600 MHz, DMSO-*d*₆) δ 10.77 (s, 1H), 8.93 (d, *J* = 8.4 Hz, 1H), 8.06 (d, *J* = 8.8 Hz, 1H), 7.95 (s, 1H), 7.94 (t, 1H), 7.63 (t, *J* = 7.7 Hz, 1H), 7.60 (d, *J* = 8.5 Hz, 1H), 7.47 (d, *J* = 15.9 Hz, 1H), 7.33 (d, *J* = 15.8 Hz, 1H), 7.03 (d, *J* = 8.4 Hz, 1H), 7.02 (s, 1H), 4.00 (s, 3H). ¹³C NMR (151 MHz, DMSO-*d*₆) δ 155.10, 152.69, 150.55, 139.66, 138.65, 134.00, 129.80, 129.15, 128.14, 125.49, 125.28, 120.90, 120.86, 119.84, 118.94, 117.18, 106.84, 48.95, 47.00, 37.98. HRMS (ESI): *m/z* calculated for C₂₁H₁₅ClN₃O⁺: 360.0903 [*M*+H]⁺, found: 360.0897.

Compound P2: Compound 4 (179 mg, 0.5 mmol) was dissolved in dry dichloromethane (10 mL). Under ice bath conditions, first 0.8 mL of triethylamine was added, then cyclopropylcarbonyl chloride (0.45 mL, 5 mmol) was slowly dripped in. After stirring the mixture at 0 °C for 2 hours, it was left to react overnight at room temperature. Upon completion of the reaction, the solvent was removed under vacuum, the residue was dissolved in ethyl acetate (15 mL), the solution was washed three times with brine, and the organic layer was dried over anhydrous sodium sulfate. Finally, the solution was concentrated under reduced pressure and purified by silica gel column chromatography (DCM:MeOH = 100:1) to yield a pale yellow solid (compound P2) of 181 mg (yield: 85%). ¹H NMR (600 MHz, DMSO-*d*₆) δ 8.93 (d, *J* = 8.4 Hz, 1H), 8.13 (s, 1H), 8.07 (d, *J* = 8.8 Hz, 1H), 7.94 (t, *J* = 7.8 Hz, 1H), 7.82 (d, *J* = 8.4 Hz, 1H), 7.68 (d, *J* = 16.0 Hz, 1H), 7.66–7.62 (t, 1H), 7.46–7.40 (m, 2H), 7.02 (s, 1H), 4.01 (s, 3H), 1.98 (m, 1H), 1.15–1.06 (m, 4H). ¹³C NMR (151 MHz, DMSO-*d*₆) δ 172.33, 152.89, 149.93, 147.60, 139.62, 137.35, 135.31, 134.13, 129.50, 128.67, 127.07, 125.61, 125.30, 125.07, 123.74, 120.84, 118.96, 107.23, 48.96, 47.74, 38.09, 12.89, 9.74. HRMS (ESI): *m/z* calculated for C₂₅H₁₉ClN₃O₂⁺: 428.1165 [*M*+H]⁺, found: 428.1156.



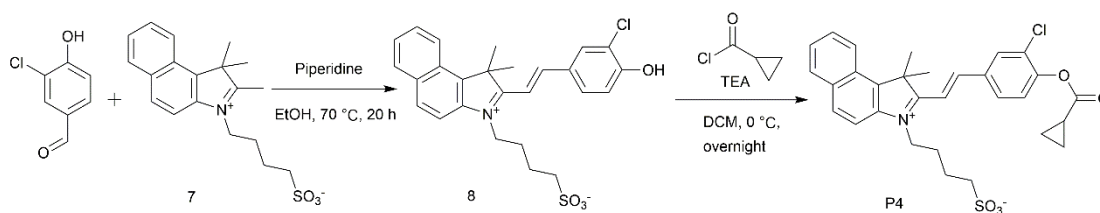
Scheme S3: Synthetic route for probe P3.

Compound 5 was synthesized according to the methods described in the literature [18].

Compound 6: Compound 5 (624 mg, 3 mmol) and 3-chloro-4-hydroxybenzaldehyde (312 mg, 2 mmol) were dissolved in acetonitrile–methanol = 1:1 (total 10 mL) with the addition of 0.5 mL of piperidine. The mixture was heated to 80 °C and stirred for 24 hours under argon protection. After the reaction was complete, the solvent was removed under vacuum. The residue was diluted with water, then extracted with DCM:isopropanol = 5:1 (3 × 10 mL). The organic layer was dried over anhydrous sodium sulfate. The solution was concentrated under reduced pressure and purified by silica gel column chromatography (DCM:MeOH = 10:1) to yield a yellow solid (compound 6) of 150 mg (yield: 22%). ¹H NMR (600 MHz, DMSO-*d*₆) δ 10.79 (s, 1H), 8.91 (d, *J* = 8.5 Hz, 1H), 8.11 (d, *J* = 8.9 Hz, 1H), 7.94–7.87 (m, 2H), 7.70 (d, *J* = 8.5 Hz, 1H), 7.60 (t, *J* = 7.7 Hz, 1H), 7.46 (d, *J* = 15.7 Hz, 1H), 7.32 (d, *J* = 15.7 Hz, 1H), 7.04 (d, *J* = 8.5 Hz, 1H), 6.99 (s, 1H),

4.56 (t, 2H), 2.53 (t, $J = 7.3$ Hz, 2H), 1.91 (m, 2H), 1.77 (m, 2H). ^{13}C NMR (151 MHz, $\text{DMSO-}d_6$) δ 162.80, 155.13, 152.64, 150.19, 139.24, 138.52, 134.17, 130.41, 128.82, 128.13, 125.48, 125.44, 121.04, 120.70, 119.20, 118.96, 117.28, 107.16, 50.62, 49.14, 46.73, 25.85, 25.11. HRMS (ESI): m/z calculated for $\text{C}_{24}\text{H}_{21}\text{ClN}_3\text{O}_4\text{S}^+$: 482.0946 $[M+2\text{H}]^+$, found: 482.0936.

Compound P3: Compound 6 (150 mg, 0.3 mmol) was dissolved in dry dichloromethane (10 mL). Under ice bath conditions, first 0.5 mL of triethylamine was added, then cyclopropylcarbonyl chloride (0.3 mL, 3 mmol) was slowly dripped in. After stirring the mixture at 0 °C for 2 hours, it was left to react overnight at room temperature. Upon completion of the reaction, the solvent was removed under vacuum, and the residue was diluted with water. The water solution was extracted repeatedly with DCM:isopropanol = 5:1 (3×10 mL), and the organic layer was dried over anhydrous sodium sulfate. The mixture was then concentrated under reduced pressure and purified by silica gel column chromatography (DCM:MeOH = 20:1) to obtain a pale yellow solid (compound P3) of 46 mg (yield: 27%). ^1H NMR (600 MHz, $\text{DMSO-}d_6$) δ 8.93 (d, $J = 8.5$ Hz, 1H), 8.18 – 8.11 (m, 2H), 7.93 (m, 2H), 7.70 (d, $J = 15.8$ Hz, 1H), 7.66–7.58 (t, 1H), 7.42 (d, $J = 15.8$ Hz, 1H), 7.39 (d, $J = 8.4$ Hz, 1H), 7.01 (s, 1H), 4.56–4.48 (t, 2H), 2.53 (t, $J = 7.2$ Hz, 2H), 2.01–1.96 (m, 1H), 1.92 (m, 2H), 1.77 (m, 2H), 1.12 (m, 4H). ^{13}C NMR (151 MHz, $\text{DMSO-}d_6$) δ 172.32, 152.85, 149.61, 147.58, 138.48, 137.92, 135.28, 134.31, 129.96, 128.57, 126.99, 125.58, 125.49, 125.03, 123.17, 121.03, 119.58, 118.99, 107.59, 50.57, 48.92, 47.76, 27.23, 22.61, 12.90, 9.73. HRMS (ESI): m/z calculated for $\text{C}_{28}\text{H}_{23}\text{ClN}_3\text{O}_5\text{S}^+$: 548.1052 $[M]^+$, found: 548.1019.



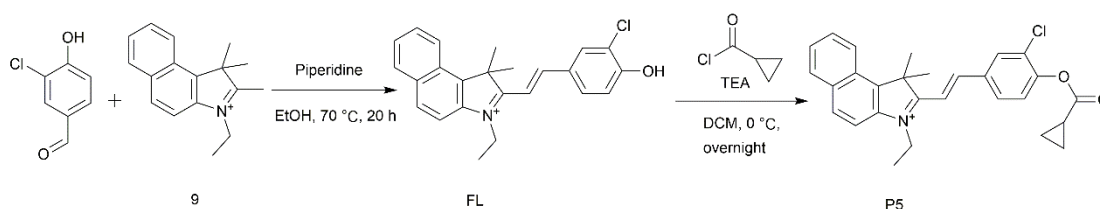
Scheme S4: Synthetic route for probe P4.

Compound 7 was synthesized according to the methods described in the literature [19].

Compound 8: Compound 7 (1038 mg, 3 mmol) and 3-chloro-4-hydroxybenzaldehyde (312 mg, 2 mmol) were dissolved in anhydrous ethanol (10 mL). An amount of 0.5 mL of piperidine was added and, under argon protection, the reaction mixture was heated to 70 °C and stirred for 20 hours. Upon completion of the reaction, the mixture was evaporated under vacuum to remove the solvent, and the residue was diluted with water. The aqueous solution was extracted with DCM:isopropanol = 10:1 (3×10 mL) and the organic layer was dried over anhydrous sodium sulfate. The mixture was concentrated under reduced pressure and purified by silica gel column chromatography (DCM : MeOH=10:1) to obtain a red solid (compound 8) of 461 mg (yield: 31.6%). ^1H NMR (600 MHz, $\text{DMSO-}d_6$) δ 11.62 (s, 1H), 8.45 (d, $J = 16.2$ Hz, 1H), 8.42 (s, 1H), 8.41 (d, $J = 8.7$ Hz, 1H), 8.27 (d, $J = 8.9$ Hz, 1H), 8.23–8.17 (m, 2H), 8.15 (d, $J = 9.0$ Hz, 1H), 7.80 (t, $J = 7.6$ Hz, 1H), 7.71 (t, $J = 7.2$ Hz, 1H), 7.66 (d, $J = 16.3$ Hz, 1H), 7.15 (d, $J = 8.5$ Hz, 1H), 4.90–4.70 (t, 2H), 2.57 (t, $J = 7.1$ Hz, 2H), 2.05 (m, 2H), 2.01 (s, 6H), 1.86 (m, 2H). ^{13}C NMR (151 MHz, $\text{DMSO-}d_6$) δ 182.56, 158.74, 152.41, 138.87, 138.61, 133.64, 133.53, 131.94, 131.45, 130.49, 128.81, 127.51, 127.49, 127.18, 123.52, 121.47, 117.62, 113.80, 110.25, 54.02, 50.59, 46.88, 27.60, 26.16, 22.64. HRMS (ESI): m/z calculated for $\text{C}_{26}\text{H}_{27}\text{ClNO}_4\text{S}^+$: 484.1349 $[M+\text{H}]^+$, found: 484.1359.

Compound P4: Compound 8 (243 mg, 0.5 mmol) was dissolved in dry dichloromethane (10 mL). Under ice bath conditions, first 0.5 mL of triethylamine was added, then cyclopropylcarbonyl chloride (0.3 mL, 3 mmol) was slowly dripped in. After stirring the mixture at 0 °C for 1 hour, it was allowed to react overnight

at room temperature. Upon completion of the reaction, the mixture was evaporated under vacuum to remove the solvent. The concentrate was dissolved in DCM (20 mL), washed with water three times, and the separated organic layer was dried over anhydrous sodium sulfate. The solution was then concentrated under reduced pressure and purified by silica gel column chromatography (DCM:MeOH = 15:1) to obtain a pale yellow solid (compound P4) of 124 mg (yield: 45%). ¹H NMR (600 MHz, CDCl₃) δ 8.41 (d, *J* = 8.3 Hz, 1H), 8.15 (d, *J* = 8.4 Hz, 1H), 8.09 (m, 2H), 8.02 (d, 1H), 8.00 (d, *J* = 8.0 Hz, 1H), 7.95 (s, 1H), 7.85 (d, *J* = 8.8 Hz, 1H), 7.71 (t, *J* = 7.4 Hz, 1H), 7.61 (t, *J* = 7.4 Hz, 1H), 7.25 (d, *J* = 8.4 Hz, 1H), 5.14–4.99 (t, 2H), 3.02 (t, *J* = 6.6 Hz, 2H), 2.28–2.18 (m, 2H), 2.12 (m, 2H), 1.99 (s, 6H), 1.88–1.82 (m, 1H), 1.19 (m, 2H), 1.11–1.02 (m, 2H). ¹³C NMR (151 MHz, CDCl₃) δ 182.68, 172.27, 151.34, 150.31, 139.02, 138.08, 133.88, 133.37, 133.29, 131.89, 130.38, 130.20, 128.49, 127.66, 127.55, 127.18, 125.03, 122.69, 113.95, 112.79, 54.00, 50.06, 47.97, 27.67, 26.51, 22.45, 12.93, 9.62. HRMS (ESI): *m/z* calculated for C₃₀H₃₁ClNO₅S⁺: 552.1611 [*M*+H]⁺, found: 552.1602.



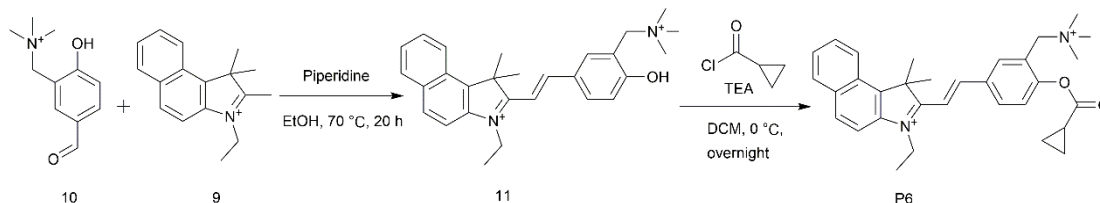
Scheme S5: Synthetic route for probe **P5**.

Compound 9 was synthesized according to the methods described in the literature [19].

Compound FL: Compound 9 (1.1 g, 3 mmol) and 3-chloro-4-hydroxybenzaldehyde (390 mg, 2.5 mmol) were dissolved in anhydrous ethanol (10 mL). An amount of 0.5 mL of piperidine was added and, under argon protection, the reaction mixture was heated to 70 °C and stirred for 20 hours. Upon completion of the reaction, the solution was evaporated under vacuum to remove the solvent. The residue was diluted with water, and the resulting solution was extracted repeatedly with DCM (3 × 10 mL). The organic layer was dried over anhydrous sodium sulfate, and after concentration under reduced pressure, it was purified by silica gel column chromatography (DCM : MeOH=15:1) to yield a dark red solid (compound FL) of 756 mg (yield: 67%). ¹H NMR (600 MHz, DMSO-*d*₆) δ 8.45–8.37 (m, 3H), 8.26 (d, *J* = 8.9 Hz, 1H), 8.19 (d, *J* = 8.2 Hz, 1H), 8.08 (d, *J* = 8.7 Hz, 1H), 8.06 (d, *J* = 9.0 Hz, 1H), 7.78 (t, *J* = 7.5 Hz, 1H), 7.69 (t, *J* = 7.5 Hz, 1H), 7.46 (d, *J* = 14.4 Hz, 1H), 7.04 (d, *J* = 8.5 Hz, 1H), 4.81–4.72 (m, 2H), 2.00 (s, 6H), 1.48 (t, *J* = 7.2 Hz, 3H). ¹³C NMR (151 MHz, DMSO-*d*₆) δ 181.28, 160.92, 151.96, 138.69, 138.15, 133.33, 133.17, 132.82, 131.42, 130.48, 128.79, 127.34, 127.27, 126.56, 123.43, 122.51, 118.33, 113.32, 108.47, 53.71, 42.21, 26.18, 14.23. HRMS (ESI): *m/z* calculated for C₂₄H₂₃ClNO⁺: 376.1462 [*M*]⁺, found: 376.1455.

Compound P5: Compound FL (376 mg, 1 mmol) was dissolved in dry dichloromethane (10 mL). Under ice bath conditions, first 0.5 mL of triethylamine was added, then cyclopropylcarbonyl chloride (0.3 mL, 3 mmol) was slowly dripped in. After stirring the mixture at 0 °C for 1 hour, it was allowed to react overnight at room temperature. Upon completion of the reaction, the mixture was evaporated under vacuum to remove the solvent. The concentrate was dissolved in DCM (20 mL) and washed with water three times. The separated organic layer was dried over anhydrous sodium sulfate, then concentrated under reduced pressure and purified by silica gel column chromatography (DCM:MeOH = 30:1) to yield a pale yellow solid (compound P5) of 368 mg (yield: 83%). ¹H NMR (600 MHz, DMSO-*d*₆) δ 8.59 (s, 1H), 8.52 (d, *J* = 16.5 Hz, 1H), 8.46 (d, *J* = 8.5 Hz, 1H), 8.34–8.30 (m, 2H), 8.24 (d, *J* = 8.2 Hz, 1H), 8.17 (d, *J* = 9.0 Hz, 1H), 7.83 (t, *J* = 7.5 Hz, 1H), 7.80–7.74 (m, 2H), 7.60 (d, *J* = 8.4 Hz, 1H), 4.90 (m, 2H), 2.03 (s, 6H), 2.00 (m, 1H), 1.54 (t, *J* = 7.3 Hz, 3H), 1.18–

1.14 (m, 2H), 1.13–1.10 (m, 2H). ^{13}C NMR (151 MHz, $\text{DMSO-}d_6$) δ 182.49, 172.18, 150.30, 149.96, 139.65, 138.49, 134.43, 133.85, 131.99, 131.67, 130.99, 130.52, 129.01, 127.98, 127.55, 127.16, 125.49, 123.78, 113.96, 113.81, 54.60, 43.38, 25.65, 14.62, 12.95, 9.91. HRMS (ESI): m/z calculated for $\text{C}_{28}\text{H}_{27}\text{ClNO}_2^+$: 444.1724 $[M]^+$, found: 444.1716.



Scheme S6: Synthetic route for probe **P6**.

Compound 10 was synthesized according to the methods described in the literature [20].

Compound 11: Compound 13 (1.1 g, 3 mmol) and compound 15 (485 mg, 2.5 mmol) were dissolved in anhydrous ethanol (10 mL). A few drops of pyridine was added and, under argon protection, the reaction mixture was heated to 70 °C and stirred for 20 hours. Upon completion of the reaction, the mixture was evaporated under vacuum to remove the solvent, the concentrate was diluted with water, the aqueous layer was extracted with DCM:isopropanol (10:1, 3 × 10 mL), the separated organic phase was dried over anhydrous sodium sulfate, concentrated under reduced pressure, and purified by silica gel column chromatography (DCM:MeOH = 15:1) to yield a dark red solid (compound 11) of 672 mg (yield: 65%). ^1H NMR (600 MHz, $\text{DMSO-}d_6$) δ 8.47 (d, $J = 16.1$ Hz, 1H), 8.44–8.37 (m, 2H), 8.33 (d, $J = 8.7$ Hz, 1H), 8.27 (d, $J = 8.9$ Hz, 1H), 8.20 (d, $J = 8.3$ Hz, 1H), 8.09 (d, $J = 8.9$ Hz, 1H), 7.80 (t, $J = 7.3$ Hz, 1H), 7.70 (t, $J = 7.5$ Hz, 1H), 7.48 (d, $J = 16.1$ Hz, 1H), 7.10 (d, $J = 8.7$ Hz, 1H), 4.81 (m, 2H), 4.56 (s, 2H), 3.14 (s, 9H), 2.02 (s, 6H), 1.49 (t, $J = 7.2$ Hz, 3H). ^{13}C NMR (151 MHz, $\text{DMSO-}d_6$) δ 181.28, 165.11, 152.56, 139.73, 138.71, 138.14, 134.95, 133.37, 131.45, 130.49, 128.84, 127.34, 125.76, 123.44, 118.41, 117.09, 113.41, 108.34, 63.09, 53.79, 52.84, 49.07, 42.42, 40.50, 26.25, 14.33. HRMS (ESI): m/z calculated for $\text{C}_{28}\text{H}_{34}\text{N}_2\text{O}^{2+}$: 207.1330 $[M]^{2+}$, found: 207.1328.

Compound P6: Compound 11 (414 mg, 1 mmol) was dissolved in dry dichloromethane (10 mL). Under ice bath conditions, first 0.35 mL of triethylamine was added, then cyclopropylcarbonyl chloride (0.2 mL, 2 mmol) was slowly dripped in. The mixture was stirred at 0 °C for 3 hours, followed by an overnight reaction at room temperature. Upon completion of the reaction, the solvent was removed from the mixture, the concentrate was dissolved in DCM (30 mL), and the solution was washed with water three times. The organic phase was dried over anhydrous sodium sulfate, then concentrated under reduced pressure and purified by silica gel column chromatography (DCM:MeOH = 20:1) to obtain a tan solid (compound P6) of 110 mg (yield: 23%). ^1H NMR (600 MHz, $\text{DMSO-}d_6$) δ 8.73 (s, 1H), 8.57 (d, $J = 16.5$ Hz, 1H), 8.51 (d, $J = 8.7$ Hz, 1H), 8.46 (d, $J = 8.5$ Hz, 1H), 8.33 (d, $J = 8.9$ Hz, 1H), 8.24 (d, $J = 8.4$ Hz, 1H), 8.18 (d, $J = 9.0$ Hz, 1H), 7.84 (m, 2H), 7.76 (t, $J = 7.5$ Hz, 1H), 7.61 (d, $J = 8.6$ Hz, 1H), 4.95 (m, 2H), 4.66 (s, 2H), 3.18 (s, 9H), 2.14–2.09 (m, 1H), 2.05 (s, 6H), 1.54 (t, $J = 7.2$ Hz, 3H), 1.18–1.10 (m, 4H). ^{13}C NMR (151 MHz, $\text{DMSO-}d_6$) δ 182.35, 172.92, 154.05, 150.99, 139.53, 138.59, 138.10, 133.84, 133.50, 132.85, 131.69, 130.55, 129.01, 127.97, 127.19, 124.93, 123.74, 121.95, 113.82, 113.53, 62.59, 54.53, 52.93, 45.95, 43.37, 40.50, 25.73, 14.63, 13.53, 10.23. HRMS (ESI): m/z calculated for $\text{C}_{32}\text{H}_{38}\text{N}_2\text{O}_2^{2+}$: 241.1461 $[M]^{2+}$, found: 241.1456.

5. NMR Spectra

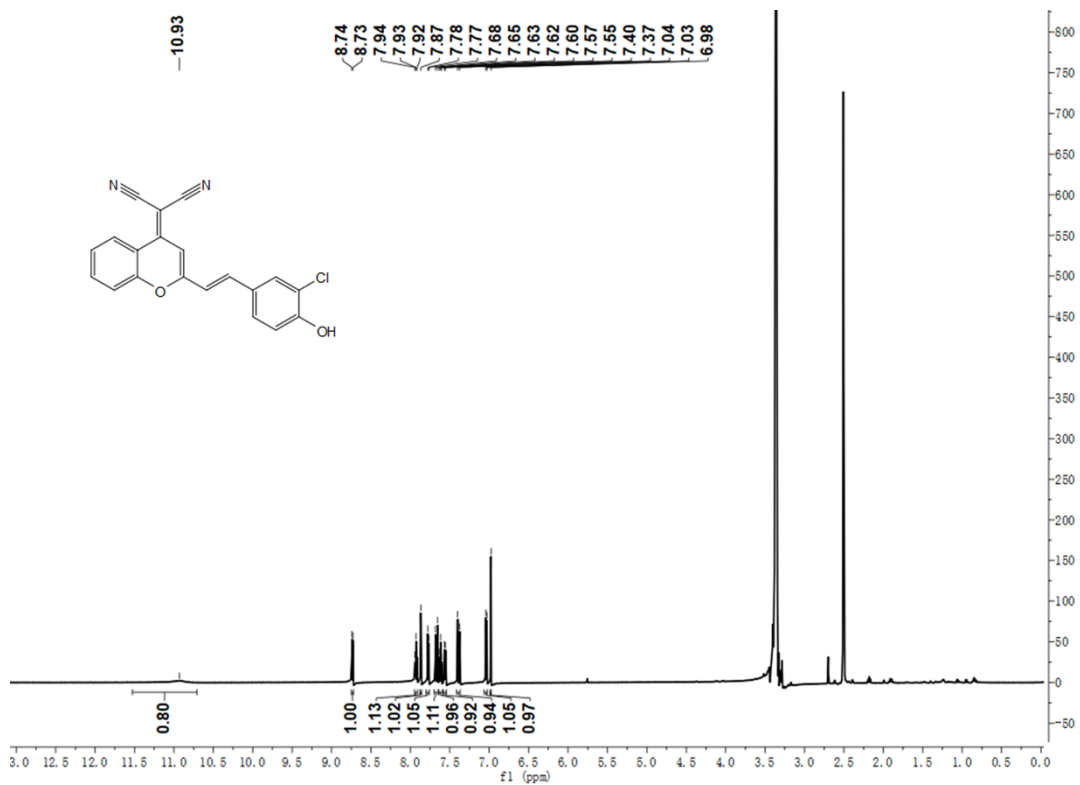


Figure S10. ¹H NMR spectra of compound 2.

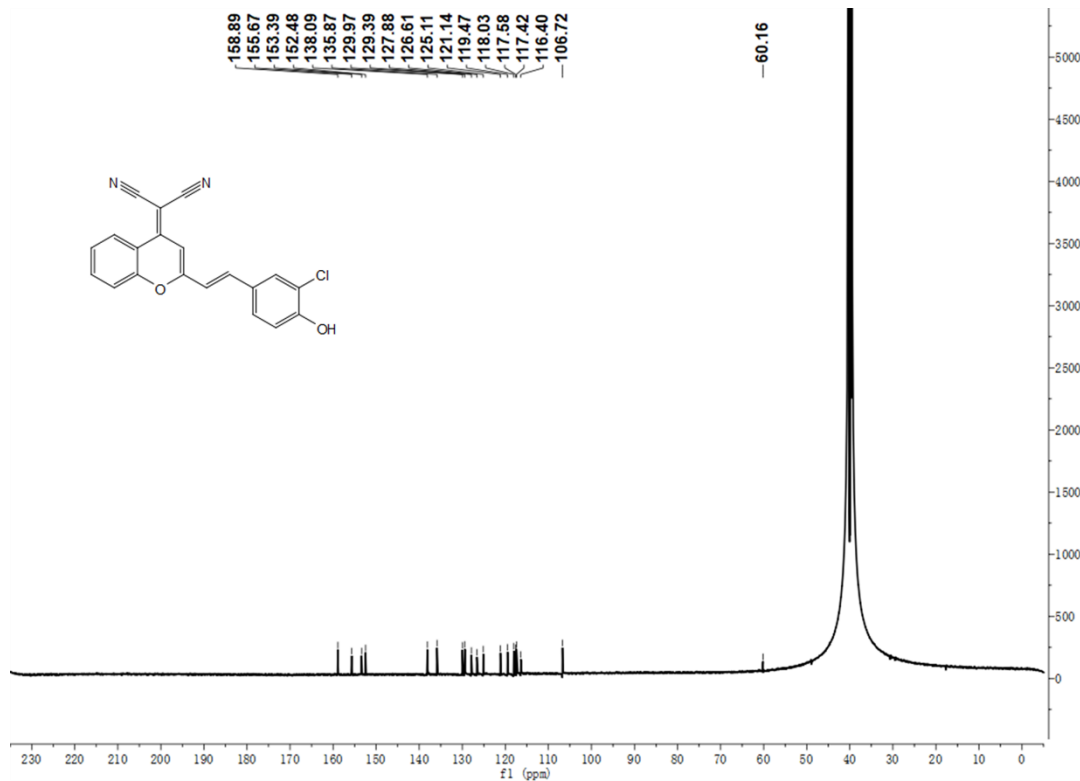


Figure S11. ¹³C NMR spectra of compound 2.

Spectrum from MASS20230901.wiff2 (sample 2) - XF4MEOH, Experiment 1, +IDA TOF MS (50 - 1000) from 0.077 to 0.134 min

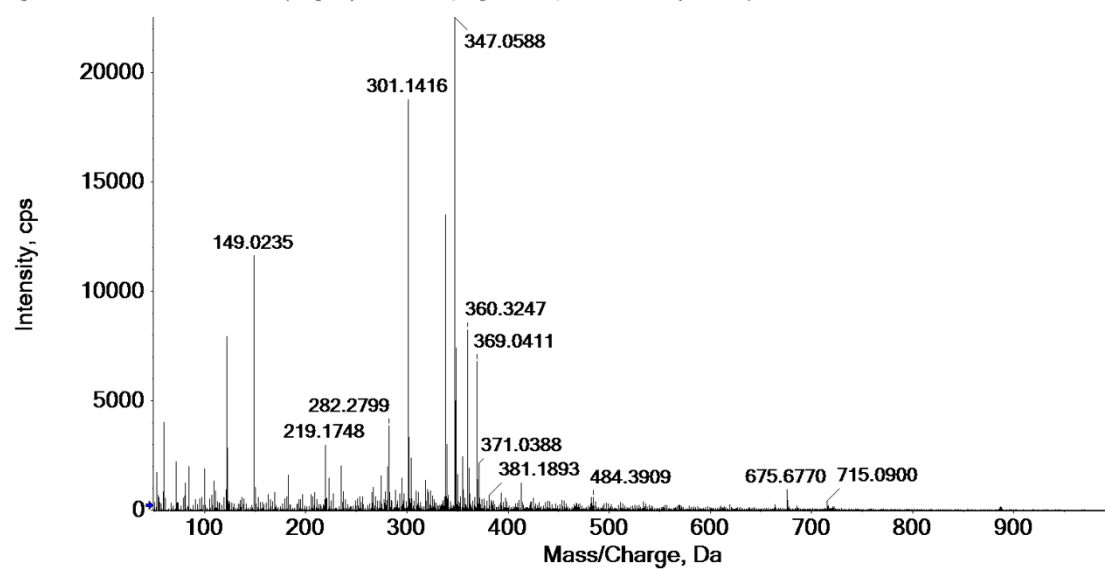


Figure S12. HRMS spectra of compound 2.

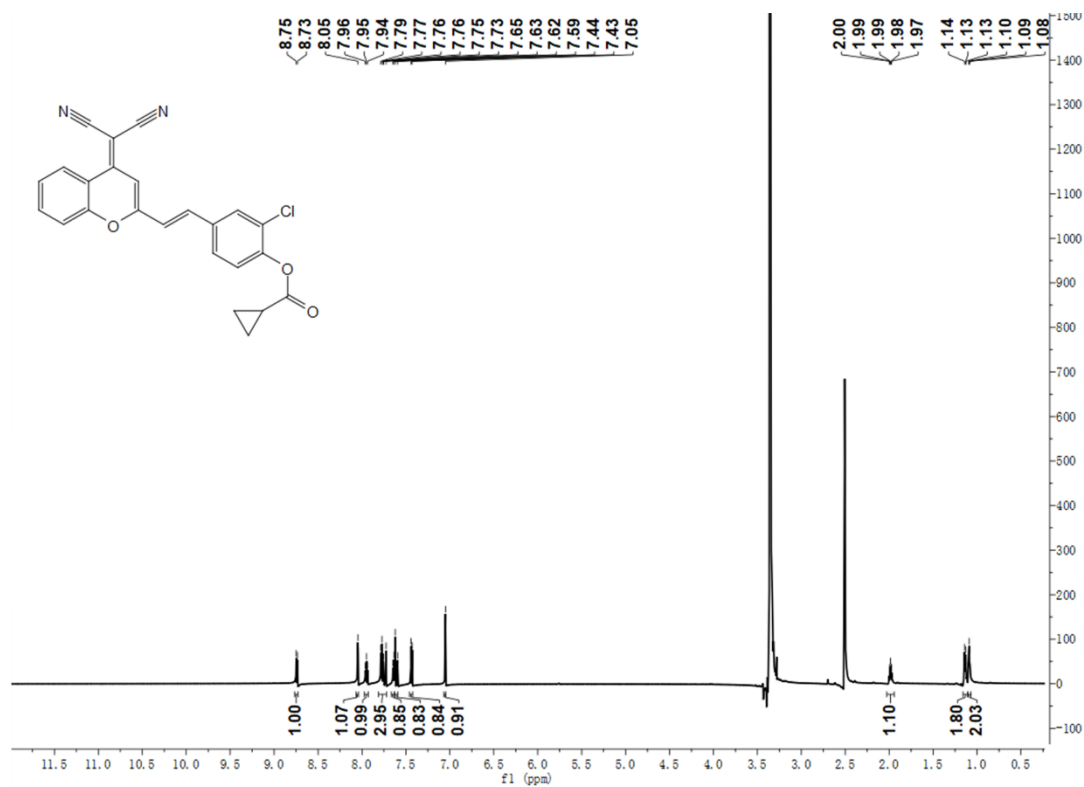


Figure S13. ¹H NMR spectra of compound P1.

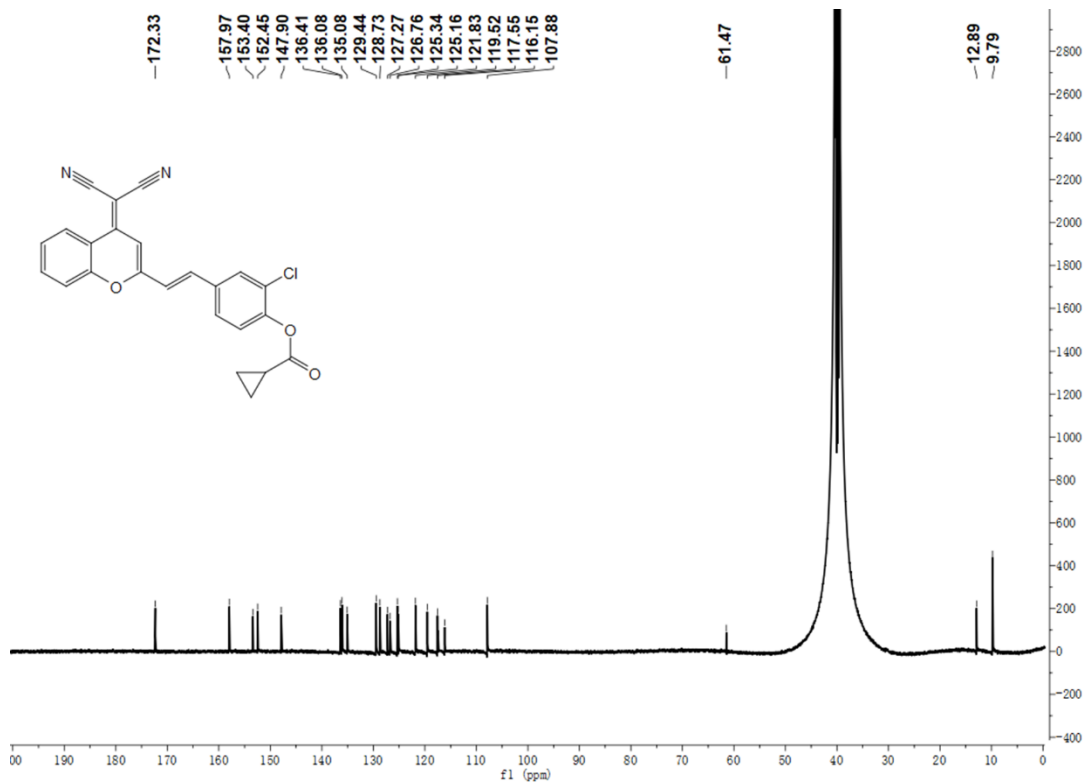


Figure S14. ¹³C NMR spectra of compound P1.

Spectrum from MASS20230901.wiff2 (sample 3) - XF5ACN, Experiment 1, +IDA TOF MS (50 - 1000) from 0.074 to 0.136 min

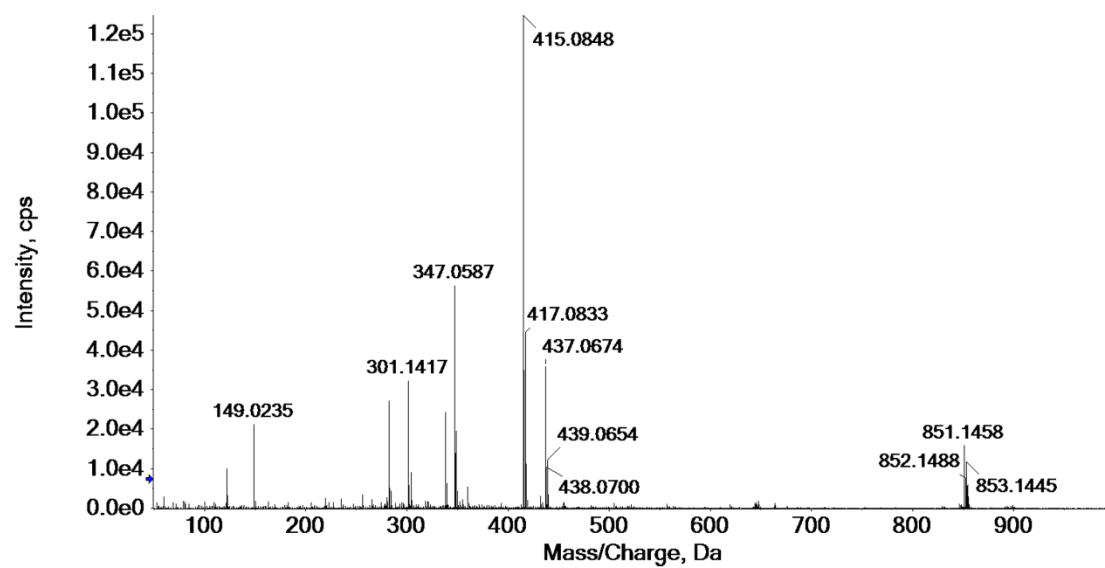


Figure S15. HRMS spectra of compound P1.

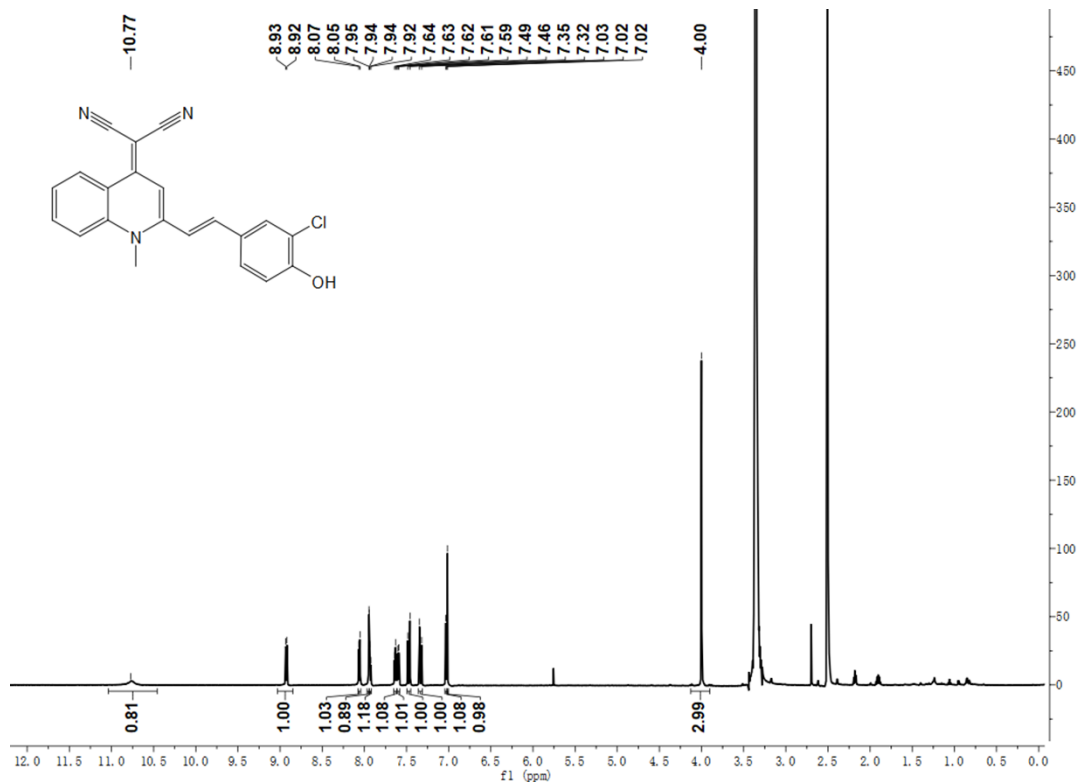


Figure S16. ¹H NMR spectra of compound 4.

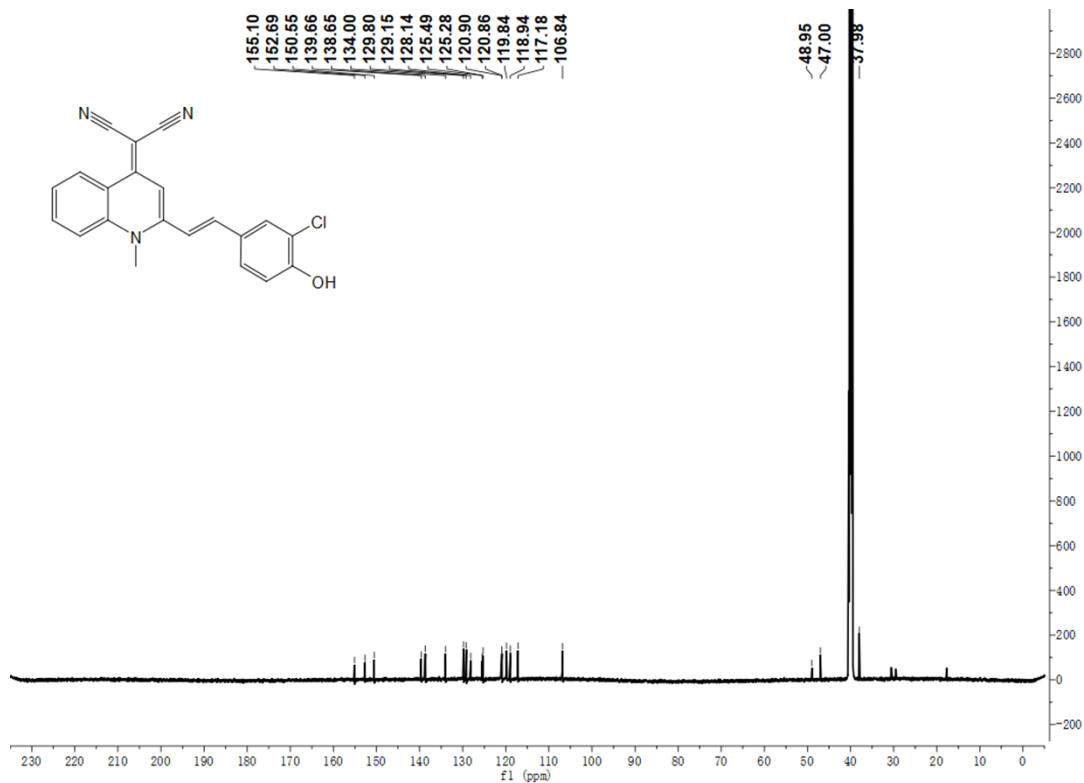


Figure S17. ¹³C NMR spectra of compound 4.

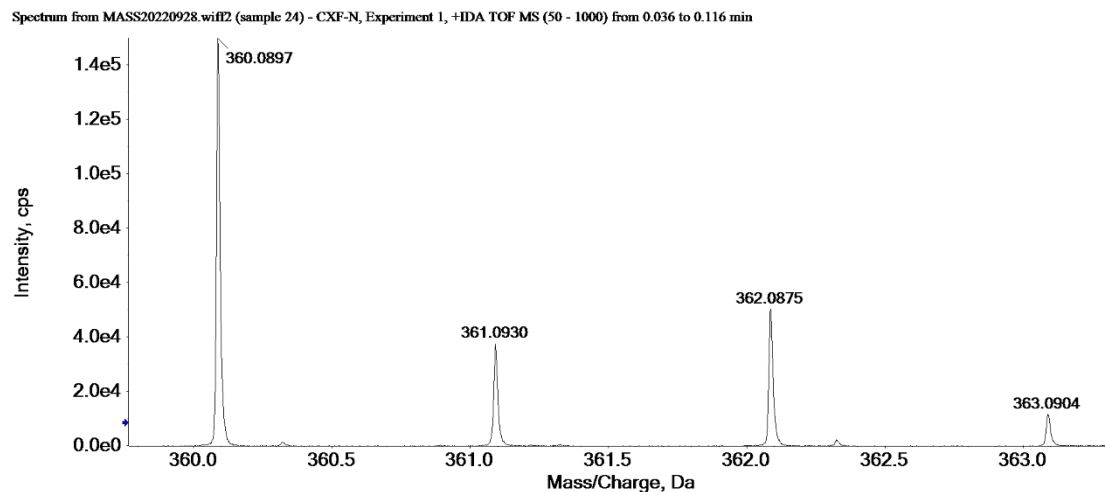


Figure S18. HRMS spectra of compound 4.

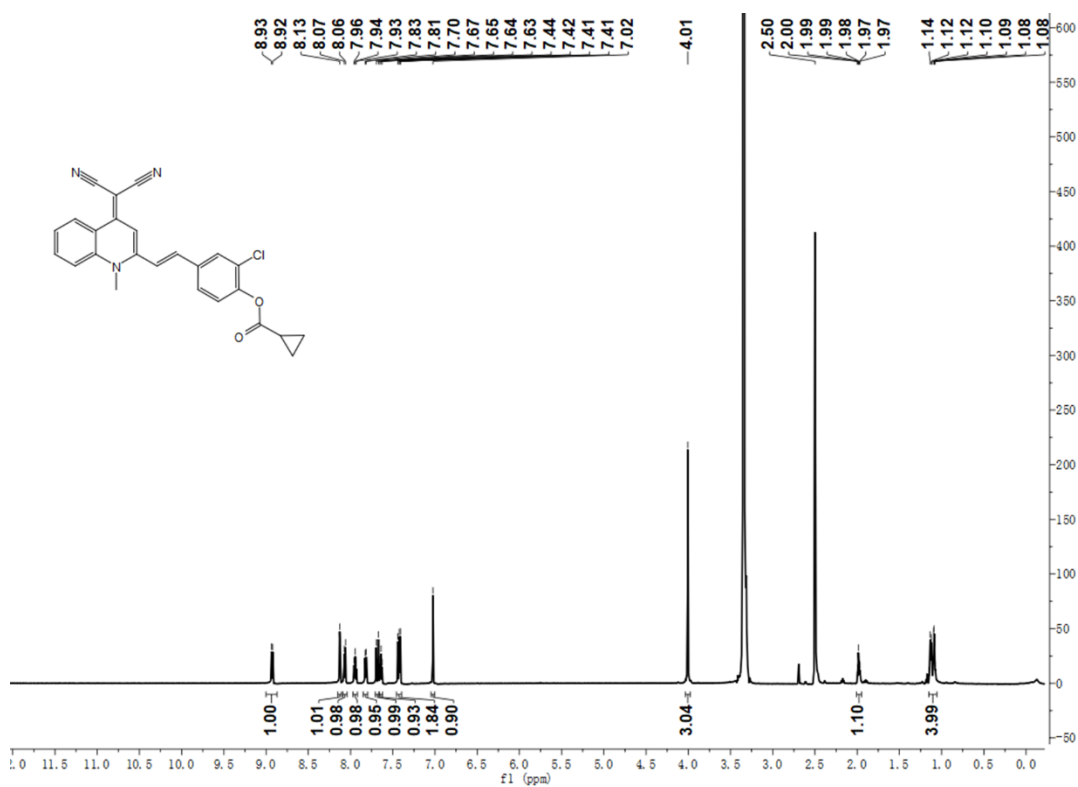


Figure S19. ¹H NMR spectra of compound P2.

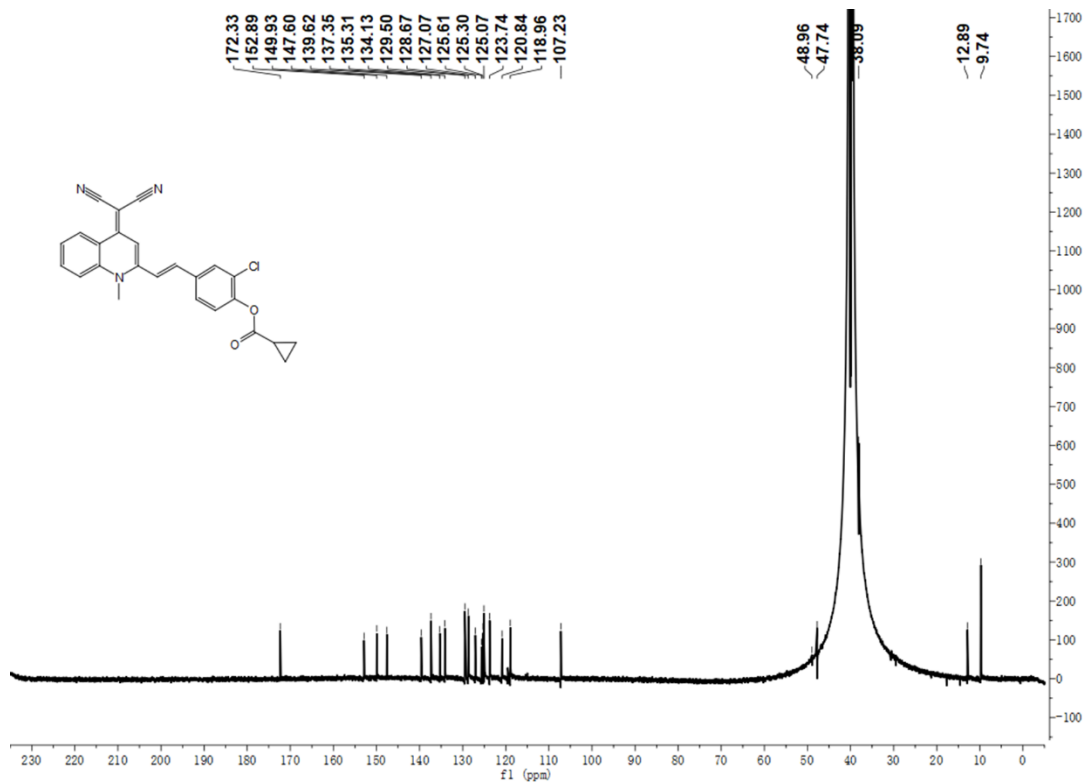


Figure S20. ^{13}C NMR spectra of compound P2.

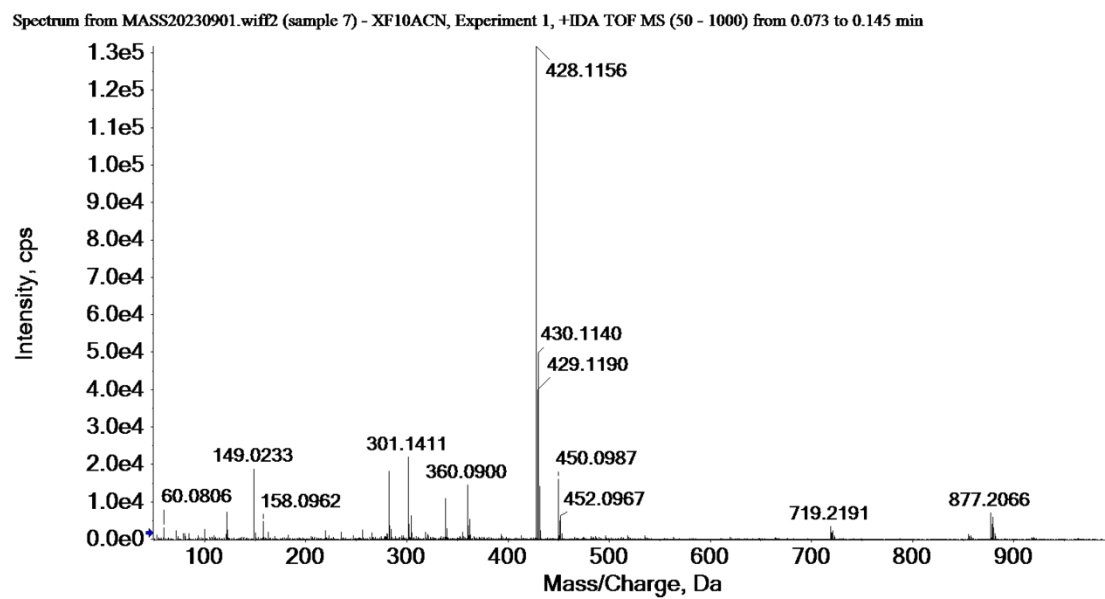


Figure S21. HRMS spectra of compound P2.

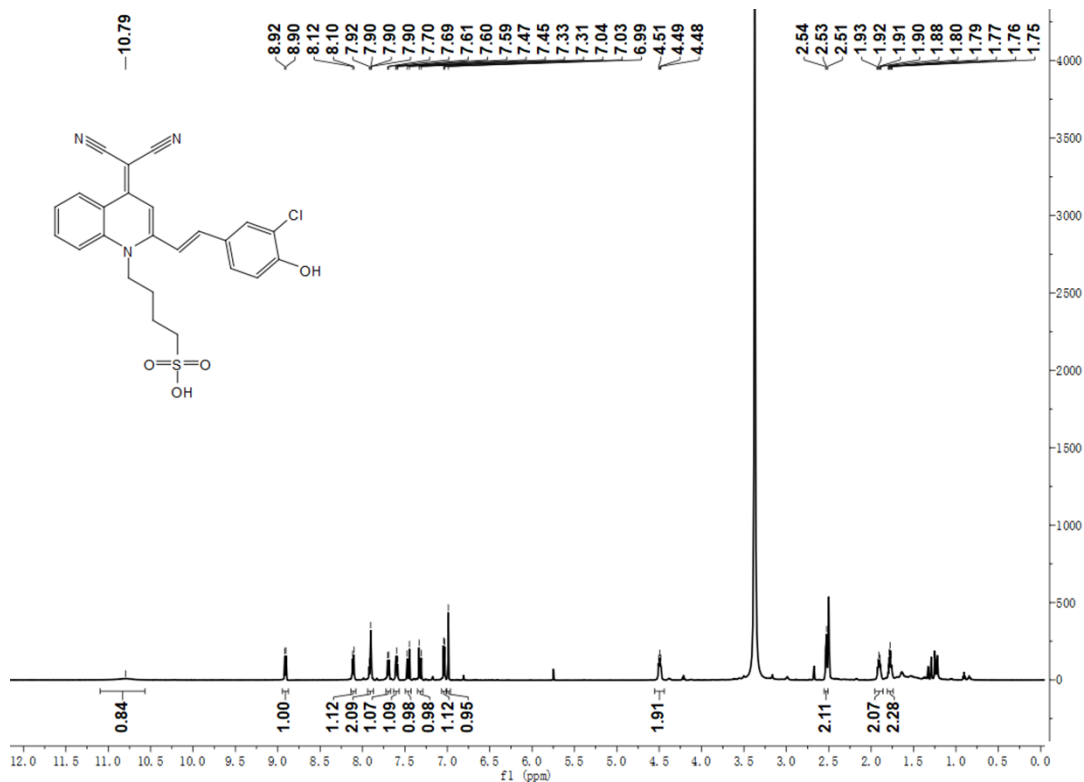


Figure S22. ¹H NMR spectra of compound 6.

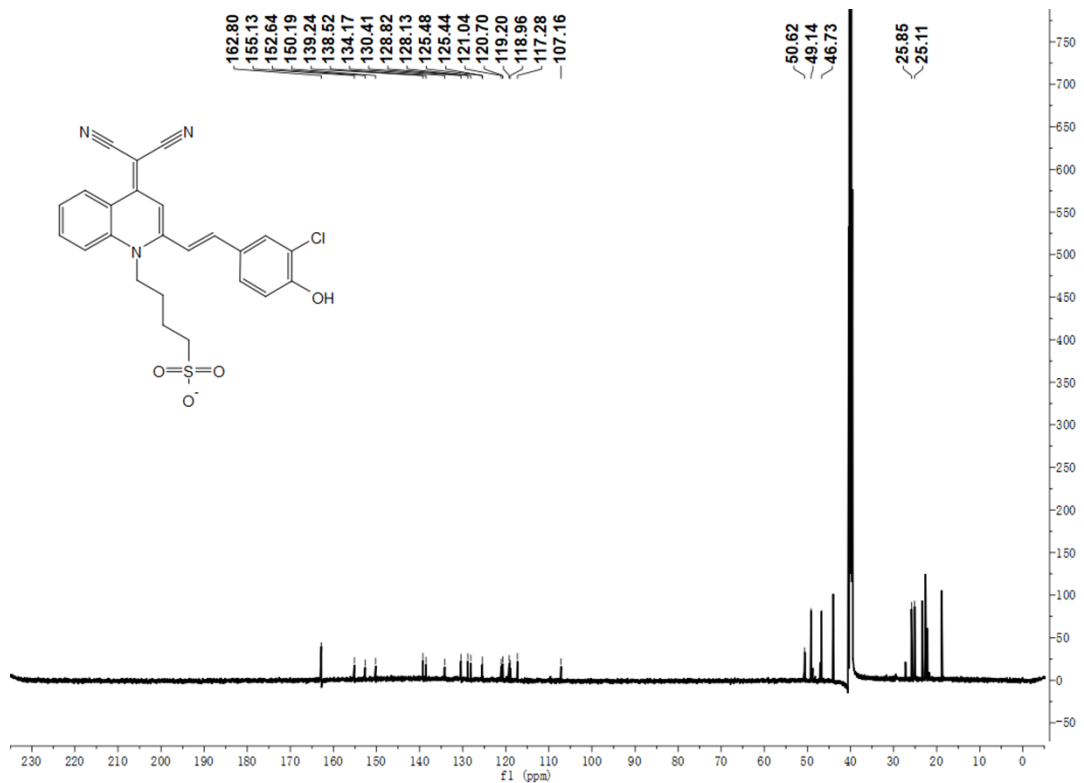


Figure S23. ¹³C NMR spectra of compound 6.

Spectrum from MASS202309182.wiff2 (sample 6) - XP918MEOH, Experiment 1, +IDA TOF MS (50 - 1000) from 0.101 to 0.214 min

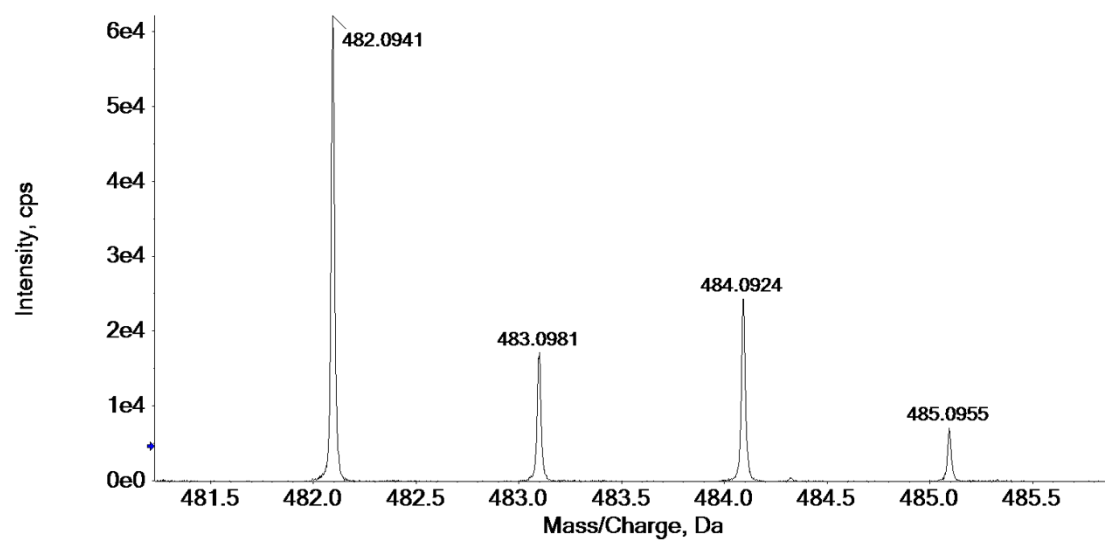


Figure S24. HRMS spectra of compound 6.

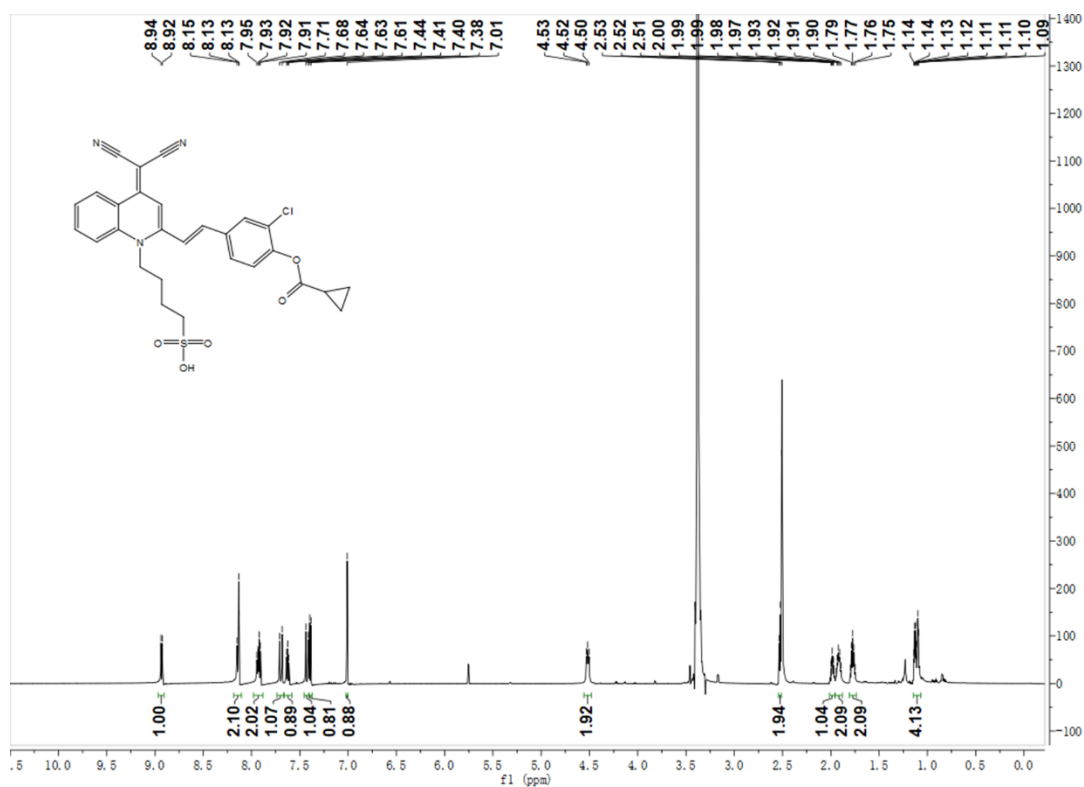


Figure S25. ¹H NMR spectra of compound P3.

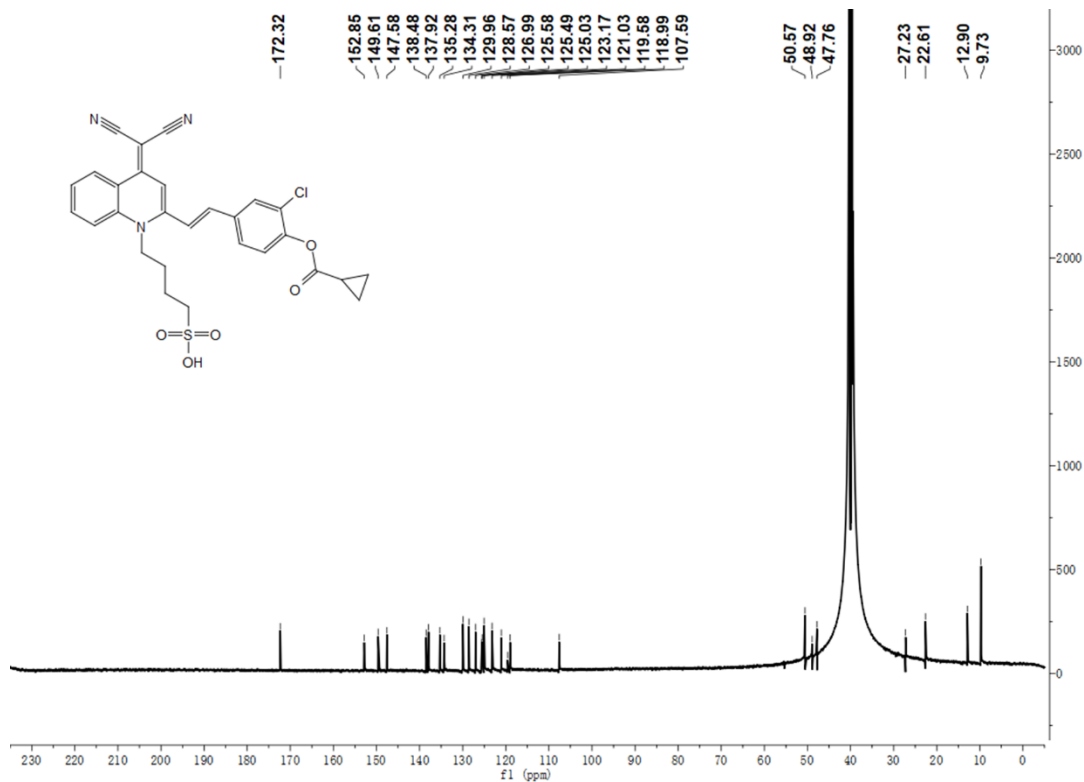


Figure S26. ^{13}C NMR spectra of compound **P3**.

Spectrum from MASS20220928.wiff2 (sample 20) - CXF-S, Experiment 1, -IDA TOF MS (50 - 1000) from 0.042 to 0.112 min

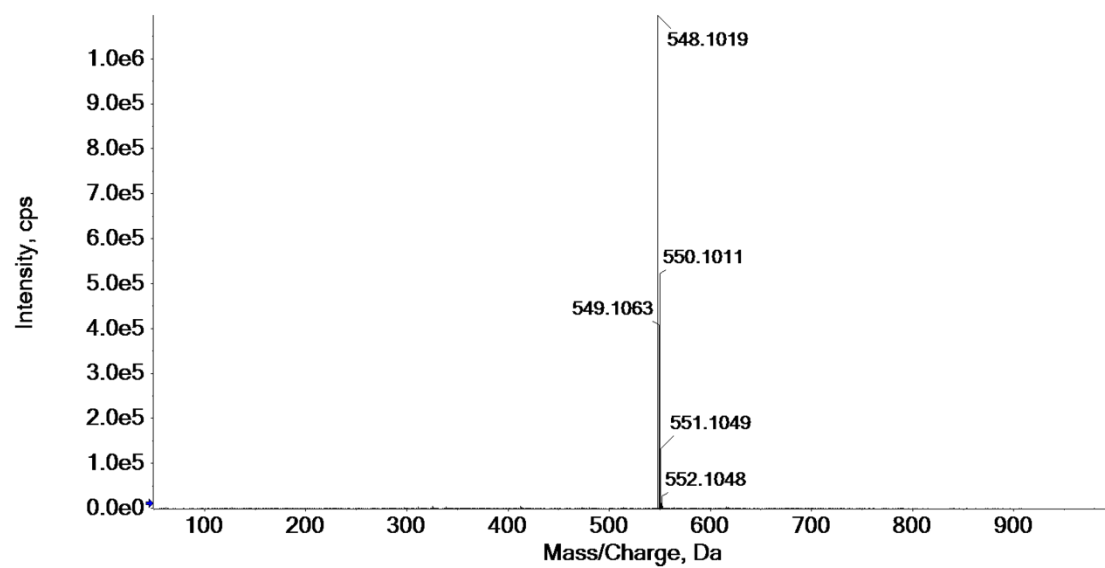


Figure S27. HRMS spectra of compound **P3**.

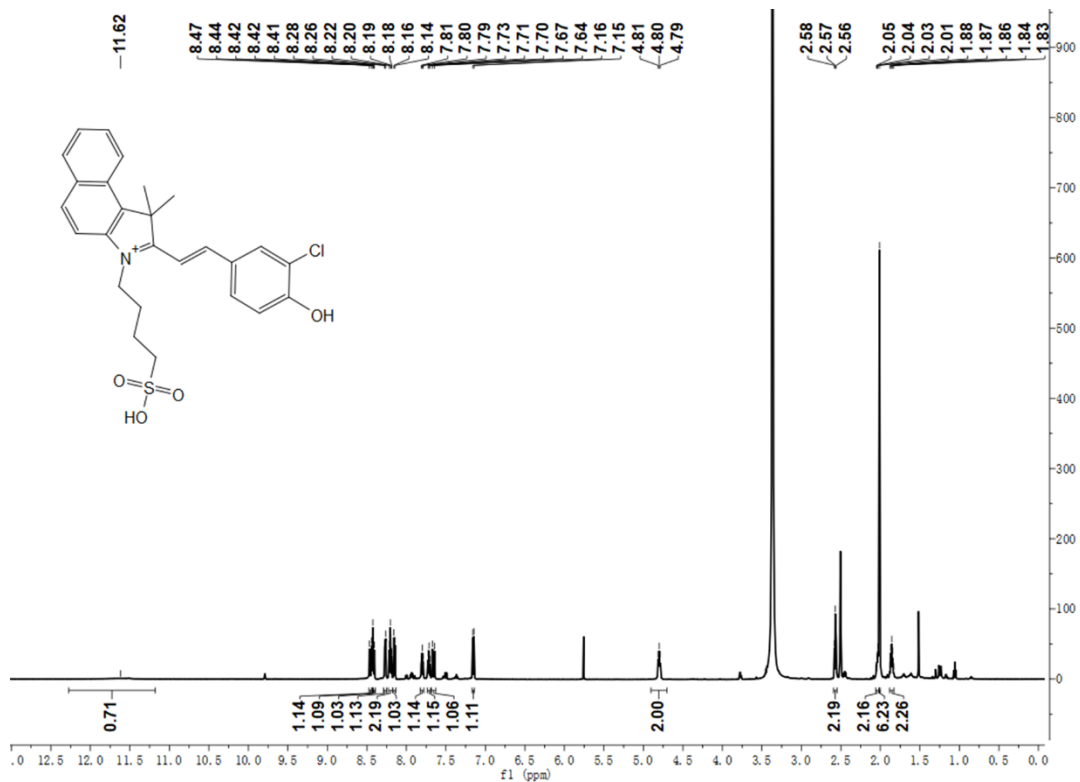


Figure S28. ¹H NMR spectra of compound 8.

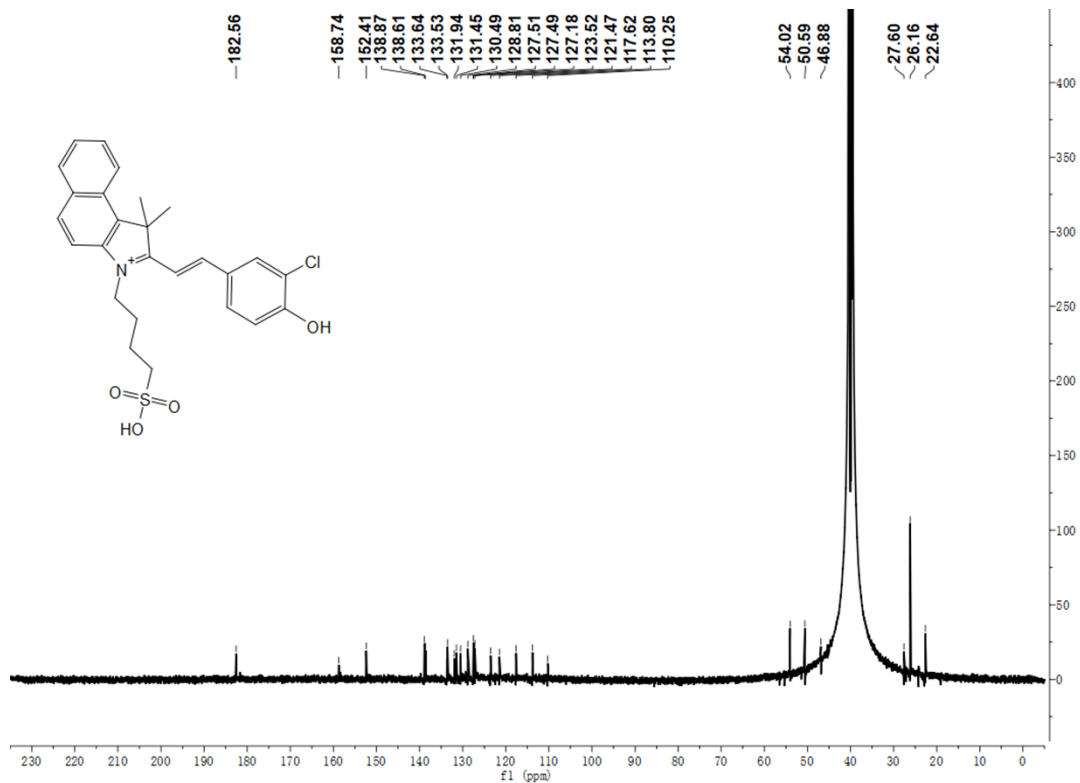


Figure S29. ¹³C NMR spectra of compound 8.

Spectrum from MASS20230901.wiff2 (sample 12) - XF17ACN, Experiment 1, +IDA TOF MS (50 - 1000) from 0.074 to 0.133 min

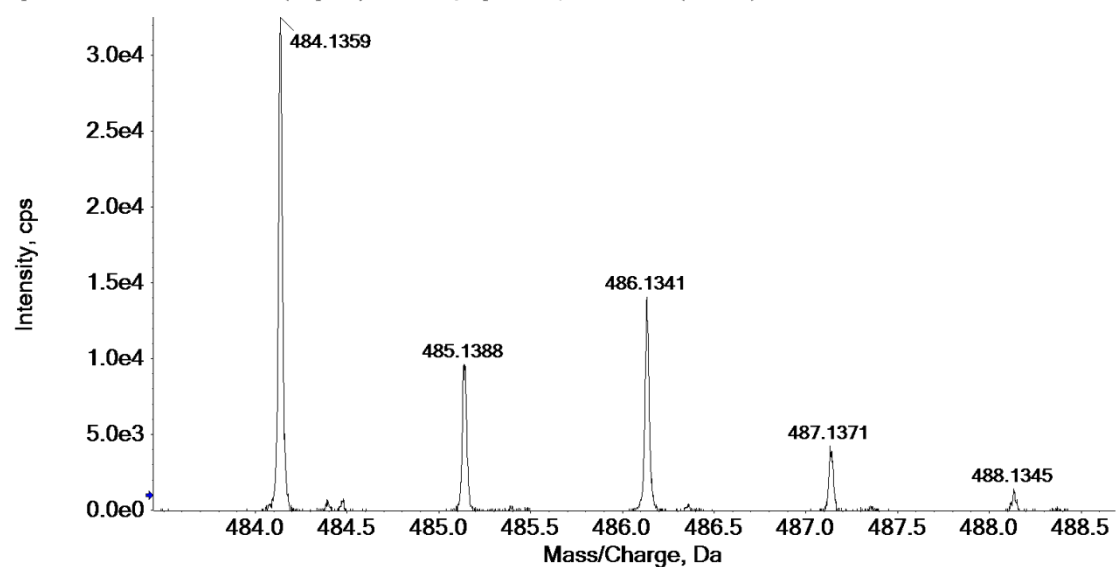


Figure S30. HRMS spectra of compound 8.

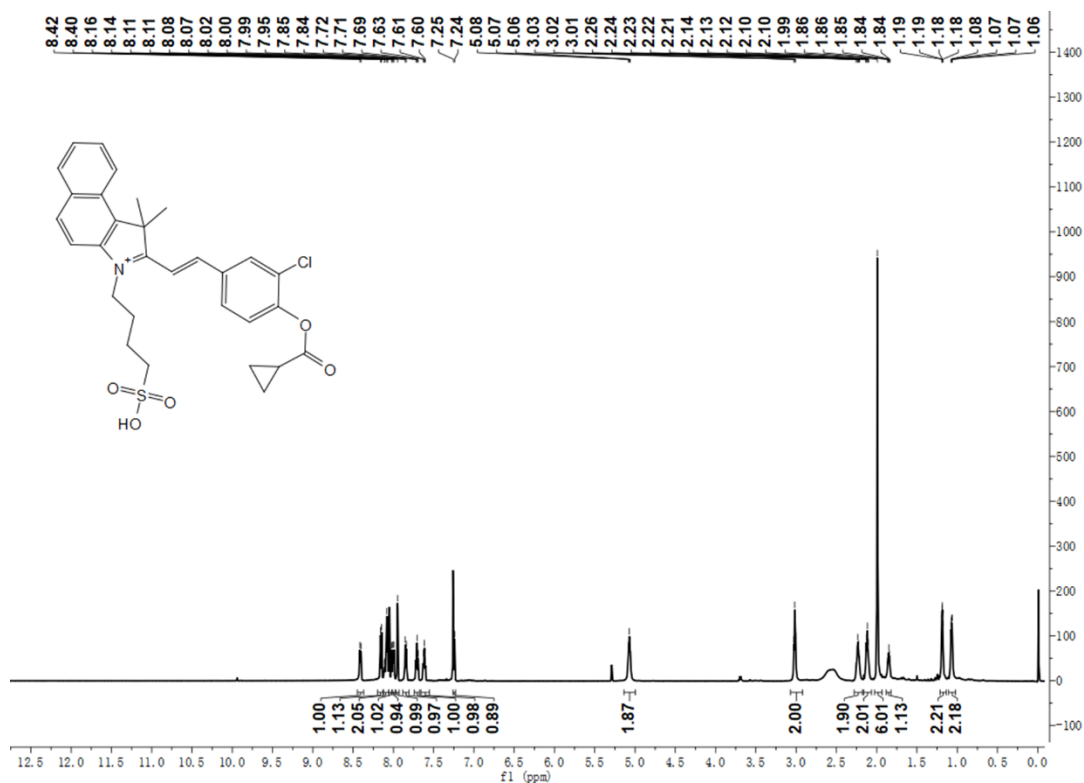


Figure S31. ¹H NMR spectra of compound P4.

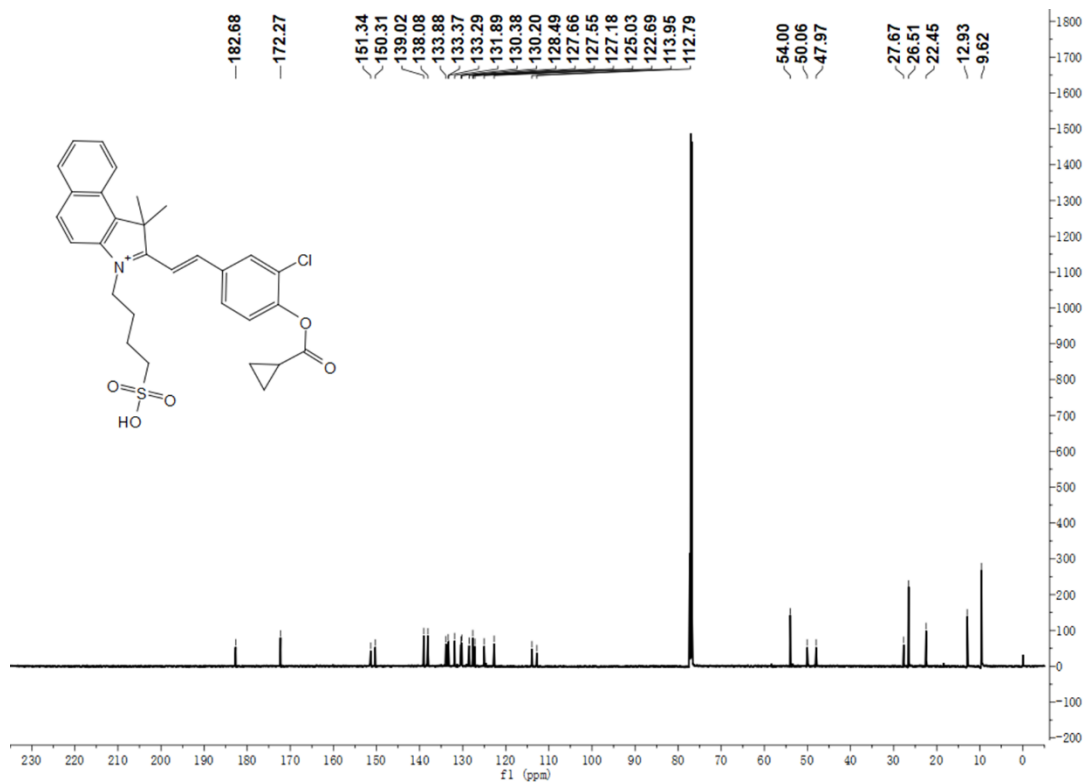


Figure S32. ¹³C NMR spectra of compound P4.

Spectrum from MASS20230522.wiff2 (sample 10) - CXF-522SO3FP, Experiment 1, +IDA TOF MS (50 - 1000) from 0.062 to 0.106 min

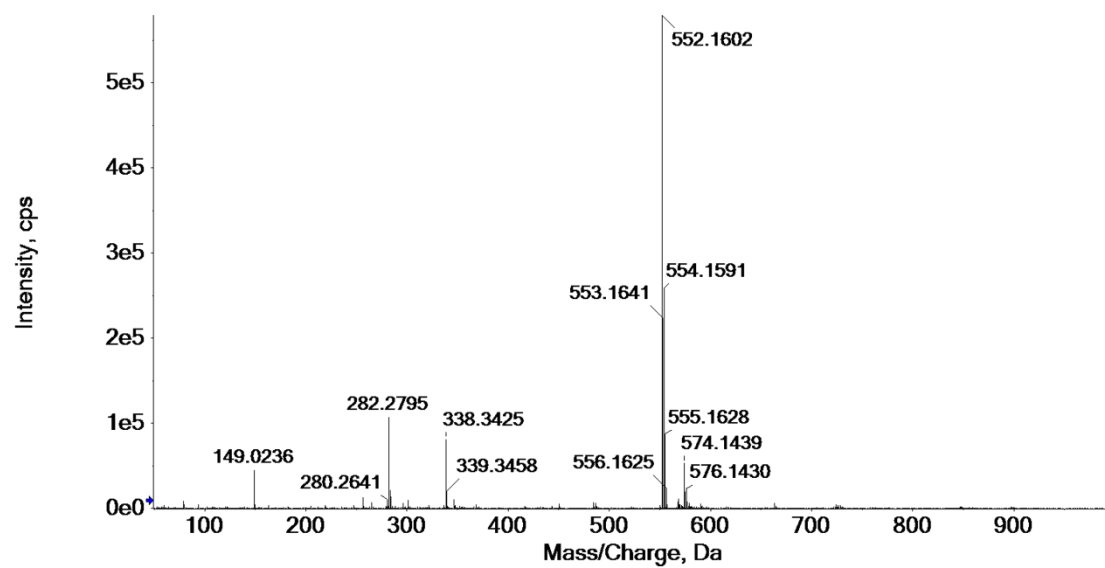


Figure S33. HRMS spectra of compound P4.

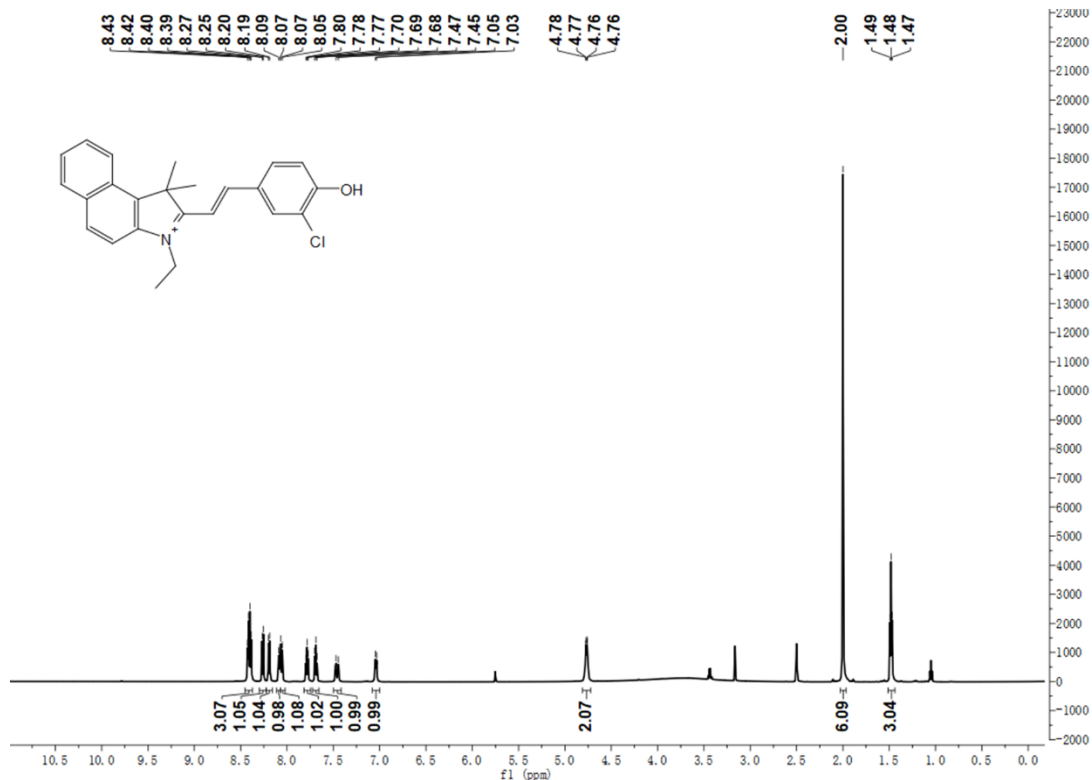


Figure S34. ^1H NMR spectra of compound FL.

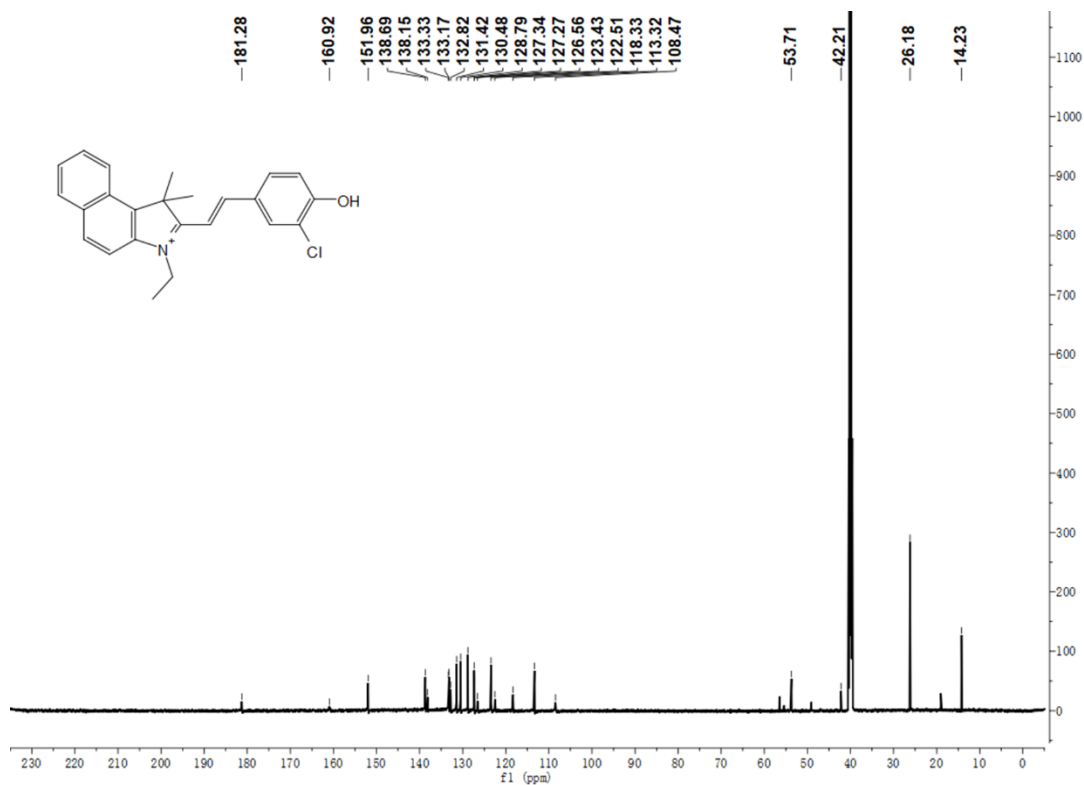


Figure S35. ^{13}C NMR spectra of compound FL.

Spectrum from MASS20230901.wiff2 (sample 10) - XF14ACN, Experiment 1, +IDA TOF MS (50 - 1000) from 0.071 to 0.137 min

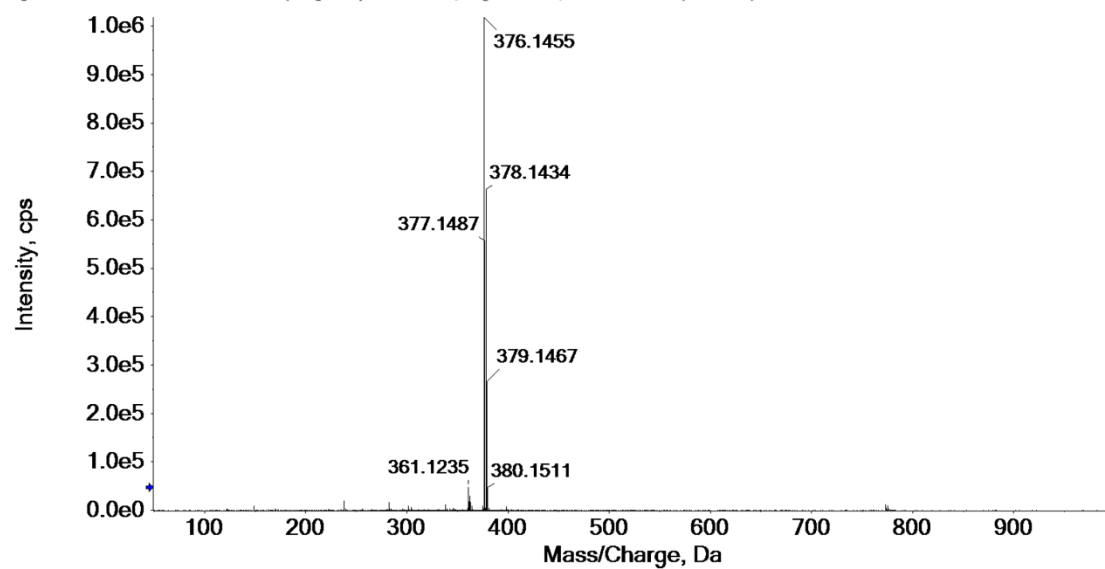


Figure S36. HRMS spectra of compound FL.

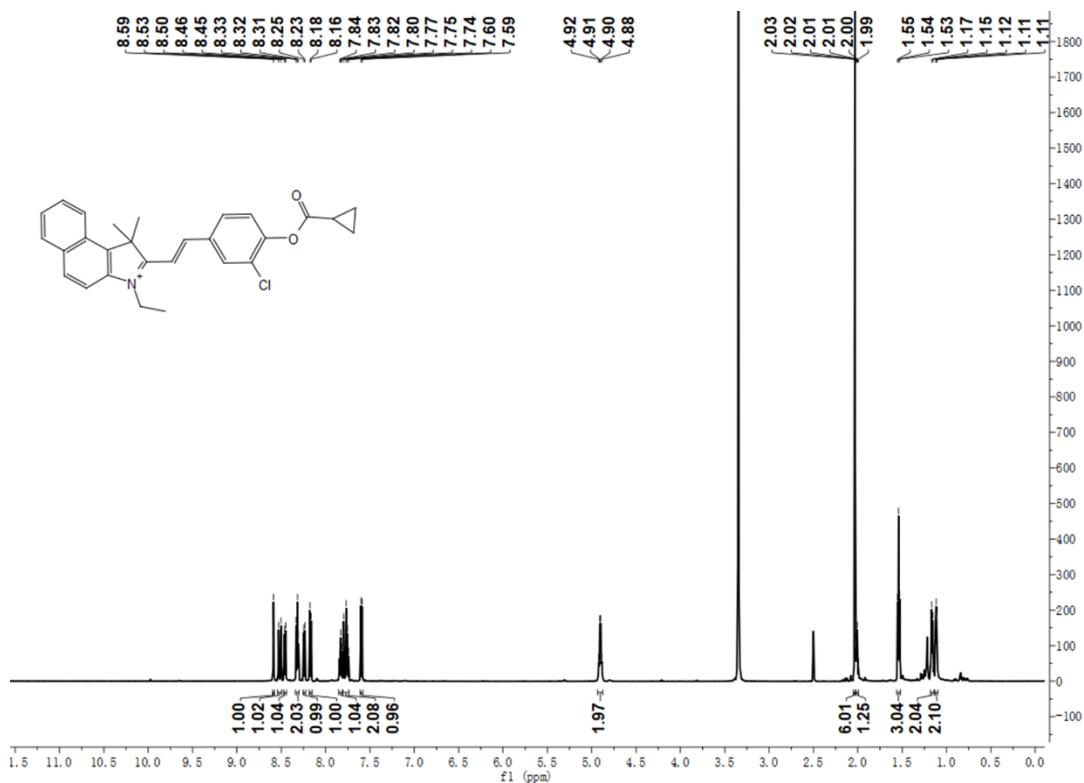


Figure S37. ¹H NMR spectra of compound P5.

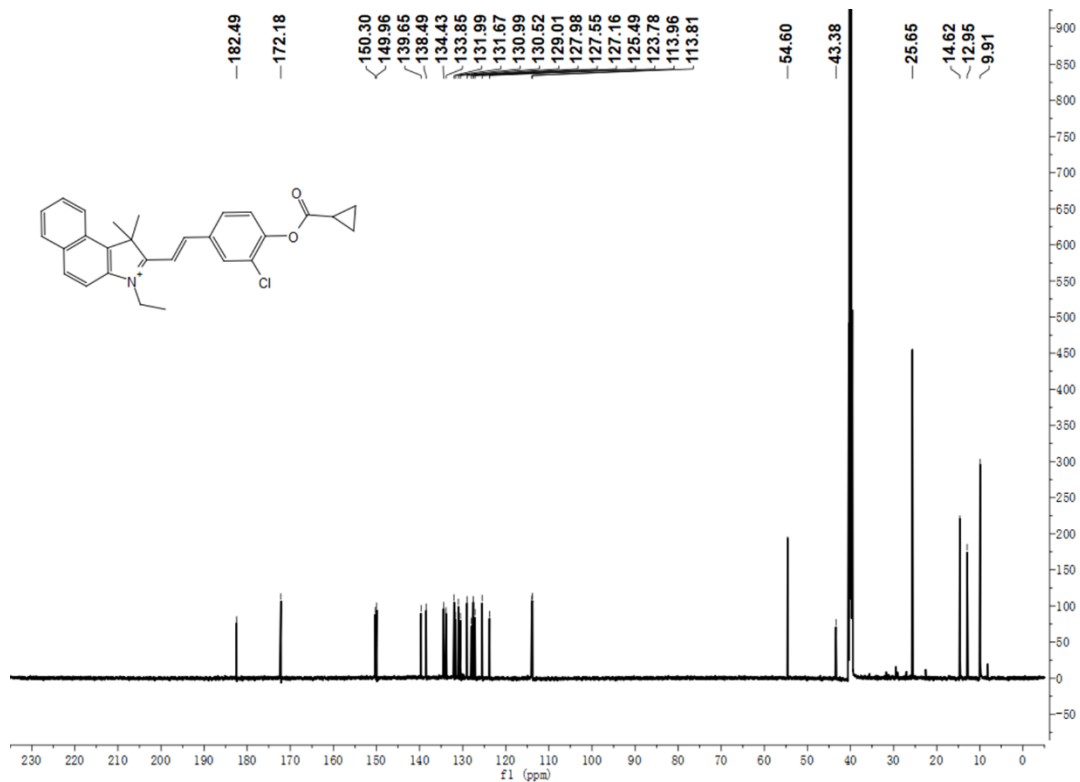


Figure S38. ^{13}C NMR spectra of compound **P5**.

Spectrum from MASS20230522.wiff2 (sample 8) - CXF-522NFP, Experiment 1, +IDA TOF MS (50 - 1000) from 0.064 to 0.114 min

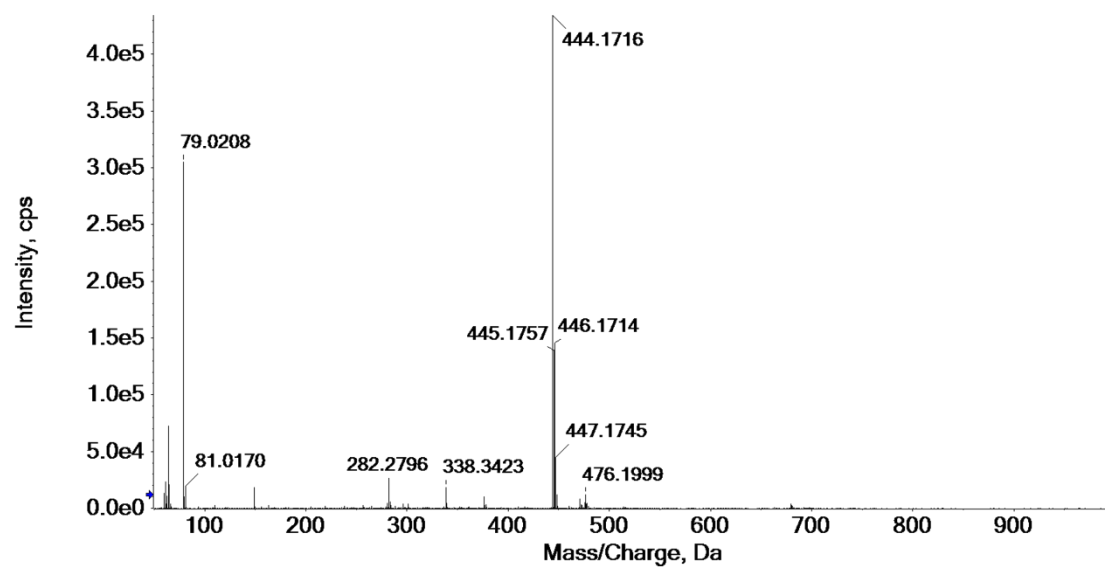


Figure S39. HRMS spectra of compound **P5**.

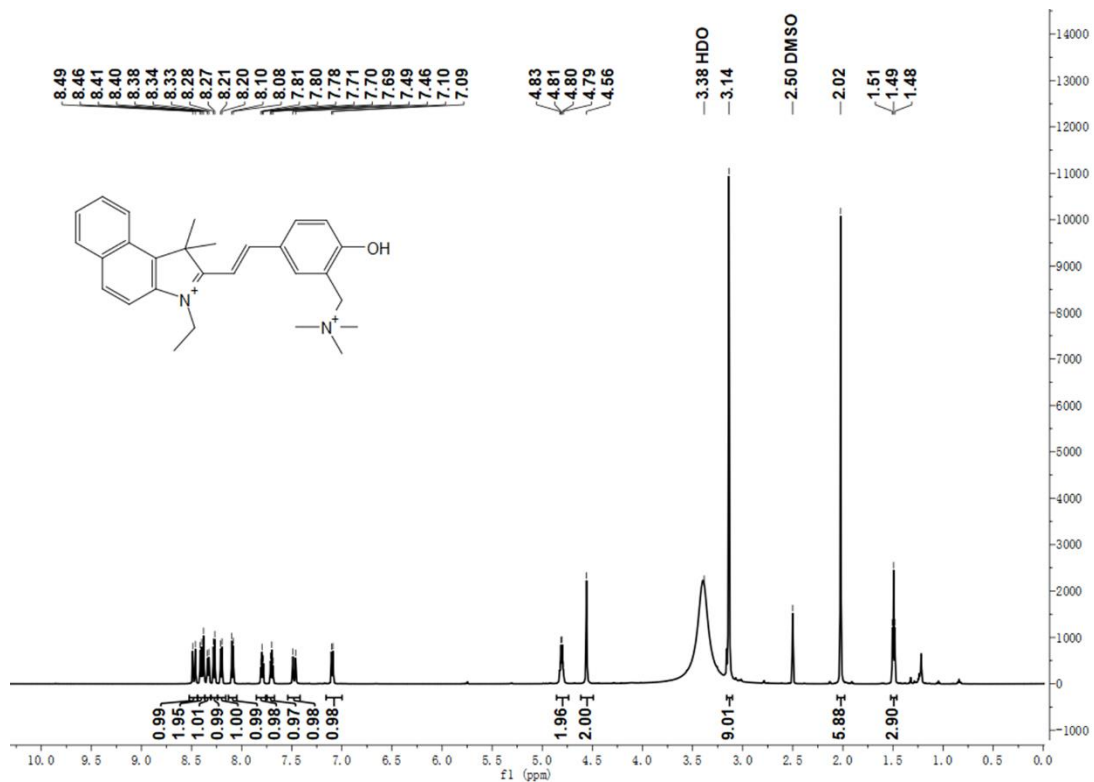


Figure S40. ¹H NMR spectra of compound 11.

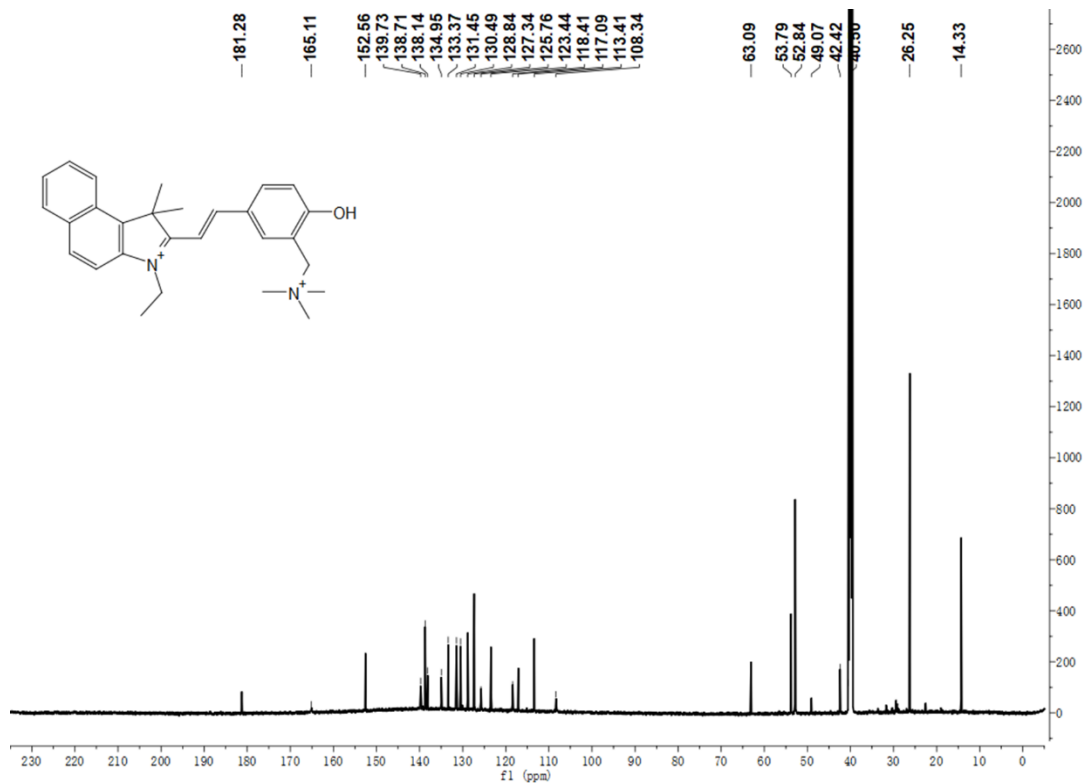


Figure S41. ¹³C NMR spectra of compound 11.

Spectrum from MASS20230522.wiff2 (sample 12) - CXF-522N3F, Experiment 1, +IDA TOF MS (50 - 1000) from 0.063 to 0.106 min

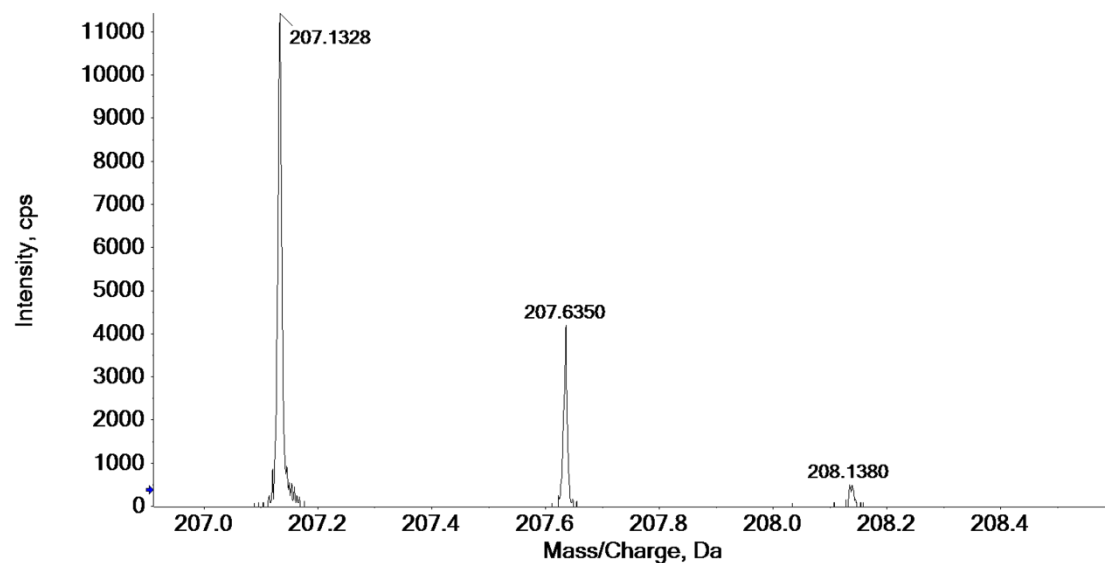


Figure S42. HRMS spectra of compound 11.

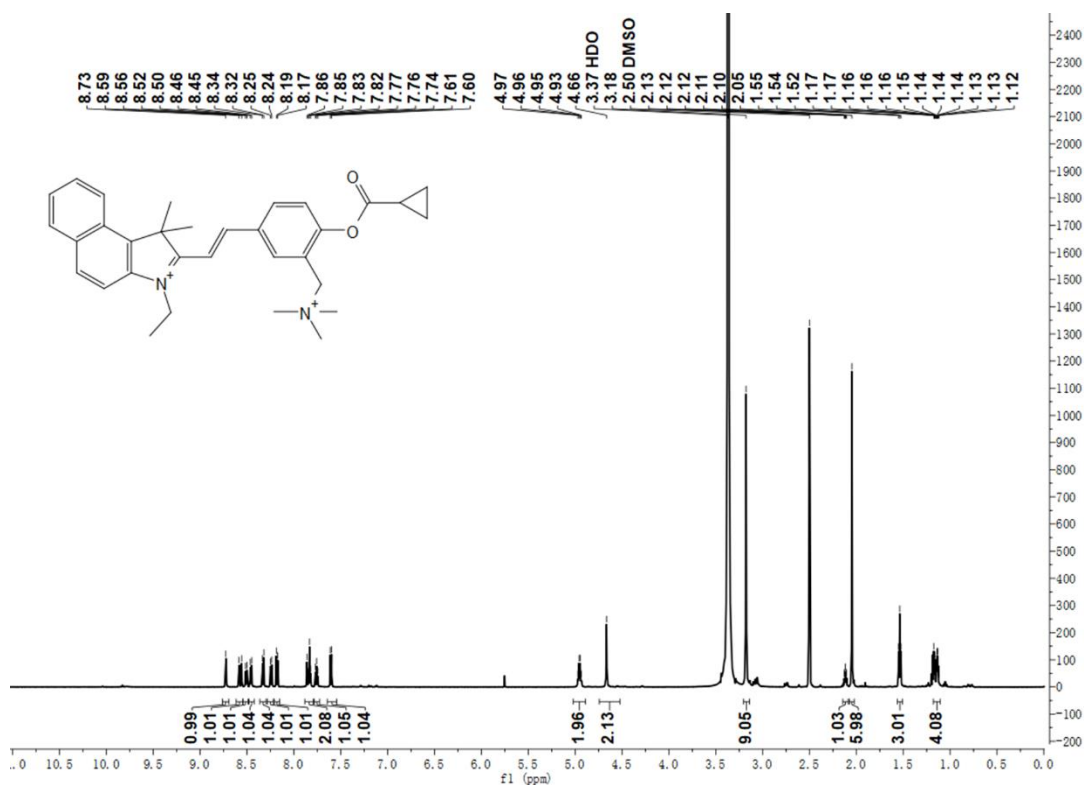


Figure S43. ¹H NMR spectra of compound P6.

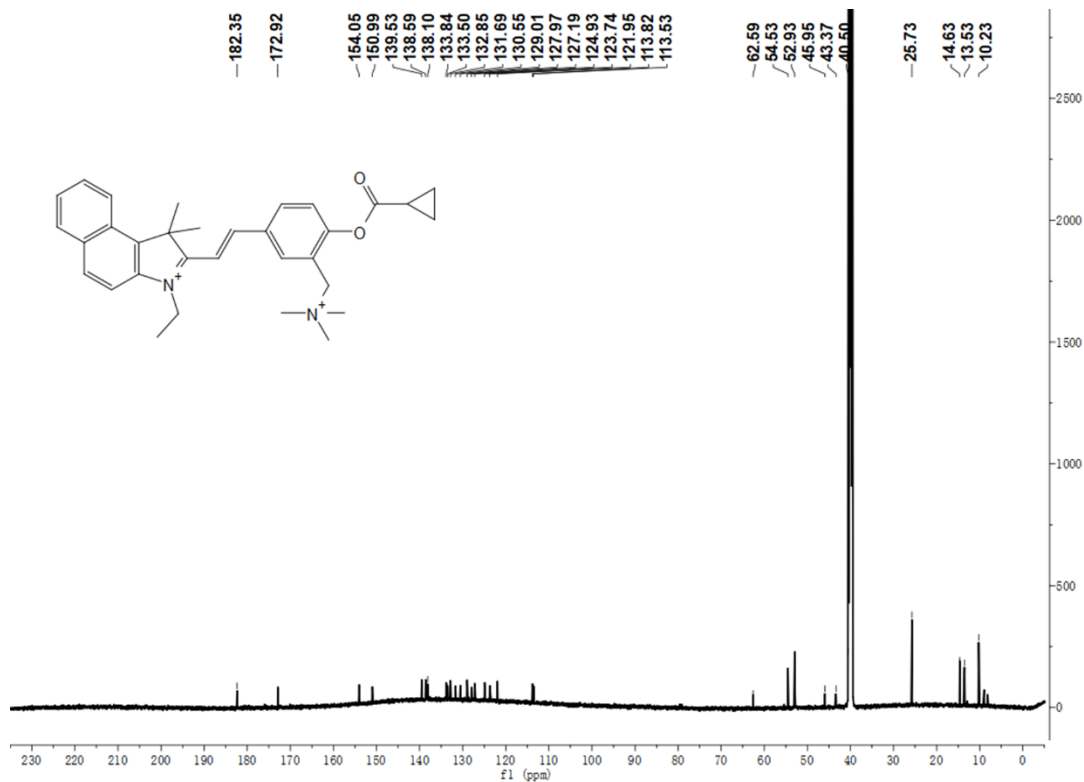


Figure S44. ^{13}C NMR spectra of compound P6.

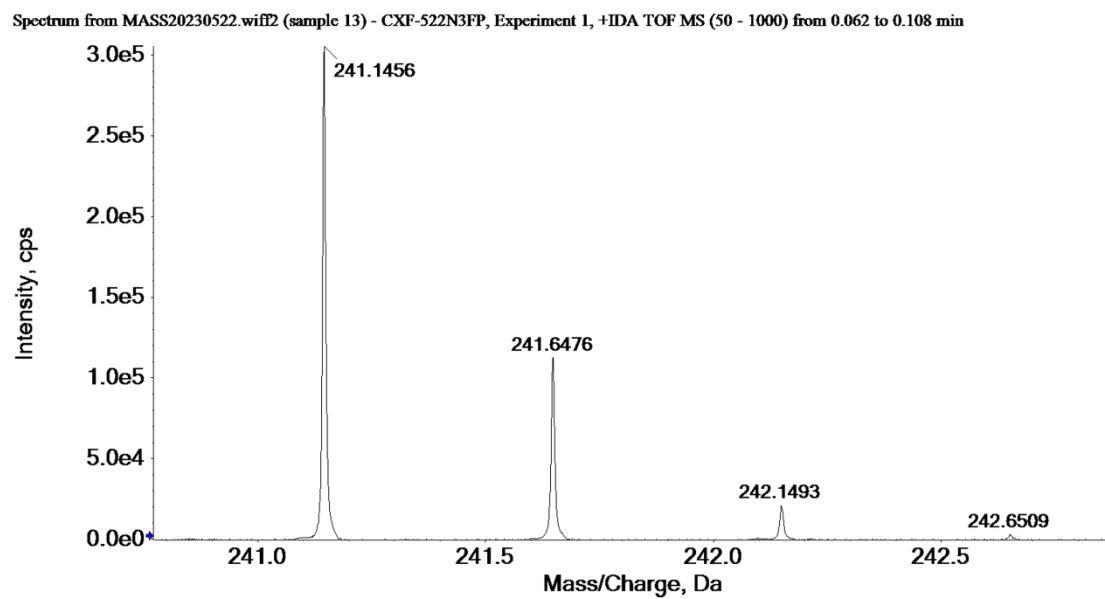


Figure S45. HRMS spectra of compound P6.

References

1. Chen, S.; Huang, W.; Tan, H.; Yin, G.; Chen, S.; Zhao, K.; Huang, Y.; Zhang, Y.; Li, H.; Wu, C. A large Stokes shift NIR fluorescent probe for visual monitoring of mitochondrial peroxynitrite during inflammation and ferroptosis and in an Alzheimer's disease model. *Analyst* **2023**, *148*, 4331-4338, doi:10.1039/D3AN00956D.
2. Ma, J.; Lu, X.; Zhai, H.; Li, Q.; Qiao, L.; Guo, Y. Rational design of a near-infrared fluorescence probe for highly selective sensing butyrylcholinesterase (BChE) and its bioimaging applications in living cell. *Talanta* **2020**, *219*, 121278, doi:<https://doi.org/10.1016/j.talanta.2020.121278>.
3. Kang, S.; Lee, S.; Yang, W.; Seo, J.; Han, M.S. A direct assay of butyrylcholinesterase activity using a fluorescent substrate. *Organic & Biomolecular Chemistry* **2016**, *14*, 8815-8820, doi:10.1039/C6OB01360K.
4. Yang, S.-H.; Sun, Q.; Xiong, H.; Liu, S.-Y.; Moosavi, B.; Yang, W.-C.; Yang, G.-F. Discovery of a butyrylcholinesterase-specific probe via a structure-based design strategy. *Chemical communications* **2017**, *53*, 3952-3955, doi:10.1039/C7CC00577F.
5. Liu, S.-Y.; Xiong, H.; Yang, J.-Q.; Yang, S.-H.; Li, Y.; Yang, W.-C.; Yang, G.-F. Discovery of butyrylcholinesterase-activated near-infrared fluorogenic probe for live-cell and in vivo imaging. *ACS sensors* **2018**, *3*, 2118-2128, doi:<https://doi.org/10.1021/acssensors.8b00697>.
6. Chen, G.; Feng, H.; Xi, W.; Xu, J.; Pan, S.; Qian, Z. Thiol-ene click reaction-induced fluorescence enhancement by altering the radiative rate for assaying butyrylcholinesterase activity. *Analyst* **2019**, *144*, 559-566, doi:10.1039/C8AN01808A.
7. Cao, T.; Zheng, L.; Zhang, L.; Teng, Z.; Qian, J.; Ma, H.; Wang, J.; Cao, Y.; Qin, W.; Liu, Y. A highly butyrylcholinesterase selective red-emissive mitochondria-targeted fluorescent indicator imaging in liver tissue of mice. *Sensors and Actuators B: Chemical* **2021**, *330*, 129348, doi:<https://doi.org/10.1016/j.snb.2020.129348>.
8. Zhang, Q.; Fu, C.; Guo, X.; Gao, J.; Zhang, P.; Ding, C. Fluorescent determination of butyrylcholinesterase activity and its application in biological imaging and pesticide residue detection. *ACS sensors* **2021**, *6*, 1138-1146, doi:<https://doi.org/10.1021/acssensors.0c02398>.
9. Zhang, P.; Fu, C.; Liu, H.; Guo, X.; Zhang, Q.; Gao, J.; Chen, W.; Yuan, W.; Ding, C. AND-logic strategy for accurate analysis of Alzheimer's disease via fluorescent probe lighted up by two specific biomarkers. *Analytical Chemistry* **2021**, *93*, 11337-11345, doi:<https://doi.org/10.1021/acs.analchem.1c02943>.
10. Wan, C.; Li, J.; Gao, J.; Liu, H.; Zhang, Q.; Zhang, P.; Ding, C. Ratiometric fluorescence assay for butyrylcholinesterase activity based on a hemicyanine and its application in biological imaging. *Dyes and Pigments* **2022**, *197*, 109874, doi:<https://doi.org/10.1016/j.dyepig.2021.109874>.
11. Xiang, C.; Xiang, J.; Yang, X.; Li, C.; Zhou, L.; Jiang, D.; Peng, Y.; Xu, Z.; Deng, G.; Zhu, B. Ratiometric imaging of butyrylcholinesterase activity in mice with nonalcoholic fatty liver using an AIE-based fluorescent probe. *Journal of Materials Chemistry B* **2022**, *10*, 4254-4260, doi:10.1039/D2TB00422D.
12. Yang, Y.; Zhang, L.; Wang, J.; Cao, Y.; Li, S.; Qin, W.; Liu, Y. Diagnosis of Alzheimer's disease and in situ biological imaging via an activatable near-infrared fluorescence probe. *Analytical Chemistry* **2022**, *94*, 13498-13506, doi:<https://doi.org/10.1021/acs.analchem.2c02627>.
13. Dong, H.; Zhao, L.; Wang, T.; Chen, Y.; Hao, W.; Zhang, Z.; Hao, Y.; Zhang, C.; Wei, X.; Zhang, Y. Dual-mode ratiometric electrochemical and turn-on fluorescent detection of butyrylcholinesterase utilizing a single probe for the diagnosis of Alzheimer's disease. *Analytical Chemistry* **2023**, *95*, 8340-8347, doi:<https://doi.org/10.1021/acs.analchem.3c00974>.
14. Shen, A.; Hao, X.; Li, M.; Zhao, Y.; Li, Z.; Hou, L.; Duan, R.; Zhang, P.; Zhang, L.; Yang, Y. Organophosphate Level Evaluation for the Poisoning Treatment by Enzyme Activation Regeneration Strategy with Oxime-Functionalized ZIF-8 Nanoparticles. *Analytical Chemistry* **2023**, *95*, 10376-10383, doi:<https://doi.org/10.1021/acs.analchem.3c01286>.
15. Wang, W.-X.; Jiang, W.-L.; Liu, Y.; Li, Y.; Zhang, J.; Li, C.-Y. Near-infrared fluorescence probe with a large stokes shift for visualizing hydrogen peroxide in ulcerative colitis mice. *Sensors and Actuators B: Chemical* **2020**, *320*, 128296, doi:<https://doi.org/10.1016/j.snb.2020.128296>.

-
16. Wang, W.-X.; Jiang, W.-L.; Mao, G.-J.; Tan, M.; Fei, J.; Li, Y.; Li, C.-Y. Monitoring the fluctuation of hydrogen peroxide in diabetes and its complications with a novel near-infrared fluorescent probe. *Analytical Chemistry* **2021**, *93*, 3301-3307, doi:<https://doi.org/10.1021/acs.analchem.0c05364>.
 17. Zhu, Z.; Wang, Q.; Liao, H.; Liu, M.; Liu, Z.; Zhang, Y.; Zhu, W.-H. Trapping endoplasmic reticulum with amphiphilic AIE-active sensor via specific interaction of ATP-sensitive potassium (KATP). *National Science Review* **2021**, *8*, nwa198, doi:<https://doi.org/10.1093/nsr/nwaa198>.
 18. Fu, W.; Yan, C.; Guo, Z.; Zhang, J.; Zhang, H.; Tian, H.; Zhu, W.-H. Rational design of near-infrared aggregation-induced-emission-active probes: in situ mapping of amyloid- β plaques with ultrasensitivity and high-fidelity. *Journal of the American Chemical Society* **2019**, *141*, 3171-3177, doi:<https://doi.org/10.1021/jacs.8b12820>.
 19. Zhang, J.; Shi, L.; Li, Z.; Li, D.; Tian, X.; Zhang, C. Near-infrared fluorescence probe for hydrogen peroxide detection: design, synthesis, and application in living systems. *Analyst* **2019**, *144*, 3643-3648, doi:10.1039/C9AN00385A.
 20. Xiang, C.; Dirak, M.; Luo, Y.; Peng, Y.; Cai, L.; Gong, P.; Zhang, P.; Kolemen, S. A responsive AIE-active fluorescent probe for visualization of acetylcholinesterase activity in vitro and in vivo. *Materials Chemistry Frontiers* **2022**, *6*, 1515-1521, doi:10.1039/D2QM00239F.